Peer-reviewed version available at Geosciences 2018, 8, 414; doi:10.3390/geosciences8110414

Present glaciers of Tavan Bogd mountain massif and their changes since the LIA

Dmitry A. Ganyushkin [1],*, Kirill V. Chistyakov [1], Ilya V. Volkov [1], Dmitry V. Bantcev [1], Elena P. Kunaeva [12], Tatyana A. Andreeva, Anton V. Terekhov [1,3], Demberel Otgonbayar[4]

[1] Institute of Earth Science, Saint-Petersburg State University, Universitetskaya nab. 7/9, Saint-Petersburg 199034, Russia; k.chistyakov@spbu.ru (K.V.C.); iliavolkov1990@gmail.com (I.V.V.);

bancev-d@yandex.ru (D.V.B.); t.andreeva@spbu.ru (T.A.A); a.terehov@spbu.ru (A.V.T.)

[2] Department of Natural Sciences and Geography, Pushkin Leningrad State University, 10 Peterburgskoe shosse, St Petersburg (Pushkin) 196605, Russia; helenkunaeva@yandex.ru

[3] Institute of Limnology RAS, Saint Petersburg, Sevastyanov st., 9 St Petersburg 196105, Russia

[4] Khovd State University of Mongolia, Institute of Natural science and technology, Hovd, Khovd province, Jargalant soum, 84000 Khovd, Mongolia Mongolian Republic

* Correspondence: d.ganyushkin@spbu.ru or Ganushkinspbgu@mail.ru; Tel.: +7-921-3314-598

Abstract

The study is based on the results of long-term field studies, satellite and aerial data analysis. In the maximum of the Little Ice Age (LIA) 243 glaciers with a total area of 353.4 km2 were reconstructed. By the results of interpretation of Corona images by 1968 the number of glaciers increased (236), the total area reduced to 242 km2. In 2010 glaciation was represented by 237 glaciers with a total area of 201 km2. Thus, from the maximum of the LIA, the glaciation of the Tavan-Bogd mountains decreased by 43%, which is somewhat less than the neighboring glacial centers (Ikh-Turgen, Tsambagarav, Tsengel-Khayrkhan and Mongun-Taiga mountains). The probable cause is the predominance of larger glaciers relatively resistant to warming and higher altitudes. The effect of glacier size on their stability is supported by differences in the relative shrinkage of glaciers in different parts of the Tavan-Bogdo-Ola massif: the smallest decline occurred in the basins of the Tsagan-Gol (31.7%) and Sangadir (36.4%) rivers where the largest glaciers are located. On the contrary, on the lower periphery of the massif, where small glaciers predominate, the relative reduction was large (74-79%). On the background of the general retreat trend large valleys glaciers retreated faster in 1968-1977 and after 2010. In 1990-s the retreat was slow. After 2010 the glacial retreat was extremely fast. The retreat of glaciers in the last 50-60 years was caused by a trend towards a decrease in the amount of precipitation until the mid-1970s and a sharp warming in the 1990s and early 2000s.

Key words

Inner Asia, Altai, glaciers, shrinkage, LIA, present dynamics

1.Introduction.

Glaciers are among the most important indicators of climate change [1], mainly of such characteristics as mean annual and summer air temperature and precipitation. It is especially important in regions with a sparse network of meteorological stations. At the same time, glaciers also act like an important climatic factor themselves, influencing the overall albedo of the Earth. Mountain glaciers, being more vulnerable to climate change than ice sheets, are the main contributors of glacier meltwater that causes rise in sea level [2]. Changes in mountain glaciers also have important implications for surface hydrology, most notably in terms of changes in runoff from glacier catchments [3], and changes in glacial lakes, which pose a serious hazard in some regions [4–6]. In arid areas meltwater from mountain glaciers can be the main source of water [7–10] [14–18]. Glacial dynamics plays important role in exogenous processes. All those factors подчеркивают важность изучения ледников и их изменений.

The longest series of observations of the dynamics of glaciers [11] cover the period from the last worldwide cooling and the culmination of glaciers known as the Little Ice Age (LIA)[12]. В то же время, Internationally coordinated glacier monitoring began in 1894, when there was already a well pronounced trend for glacial retreat [11]. As a result, there are few direct estimations of the positions of the glaciers in the maximum of the LIA, mostly in the Alps [13]. However, it is usually possible to reconstruct the glaciation of the LIA maximum on the geomorphological basis [14]. Post-LIA glacial retreat, starting in the interval 1800-1850 was uneven. For example, in the Alps end moraines were formed 1890, 1920, and 1980 AD, during short oscillations or episodes of glacier standstill [15], [16]. Finally, the last several dozen years are a period of global acceleration of the glacial retreat. Glaciological and geodetic observations show that the rates of early 21st-century mass loss are without precedent on a global scale, at least for the time period observed [17].

Though the pattern of glacial dynamics after the LIA maximum is relatively well known in several humid areas (the Alpes [16,18,19], Scandinavia [20–22] etc.) there is still less information about the arid intracontinental areas, which are usually remote sensing and paleoreconstructions ([14,23–27].

Tavan Bogd mountain massif (fig. 1) is situated in one of such remote intracontinental arid areas. It is the largest center of Altai glaciation. At this point, the mountain ranges of the Southern Altai from the west, Sailugem from the north-east and the Mongolian Altai from the south converge. The watershed ridge in the northern part of the massif separates Argut river basin from Irtysh river basin, located to the southwest of it, and from Kobdo river Basin (internal drainage zone), located to the south-east. The northern part (the territory of Russia) is weakly dissected and gentle sloped, the foot of the massif here is the highest (2000-2400 m, Ukok plateau). Five dome-shaped peaks, whose height reaches 4,000 m (the highest point is the Russkiy Shater (Russian Tent) – 4,134 m a.s.l.) are situated here. On the contrary, the western and eastern slopes of the massif are distinguished by strong dissection and have a pronounced alpine type of relief. Deep troughs with hanging valleys of tributaries are framed by crests up to 4,000 m and higher (Khuiten Uul (Cold Mountain, 4,374 m asl, the highest mountain in Mongolia, Burged (Eagle, 4,310 m asl), Naran (Sunny, 4,280 m asl), Olgii (Motherland, 4,100 m asl), and Malchin (Herdsman, 4,050 m asl). 2,600 km^2.

Preprints (www.preprints.org) | NOT PEER-REVIEWED | Posted: 18 August 2018 doi:10.20944/preprints201808.0332.v1

Peer-reviewed version available at Geosciences 2018, 8, 414; doi:10.3390/geosciences8110414

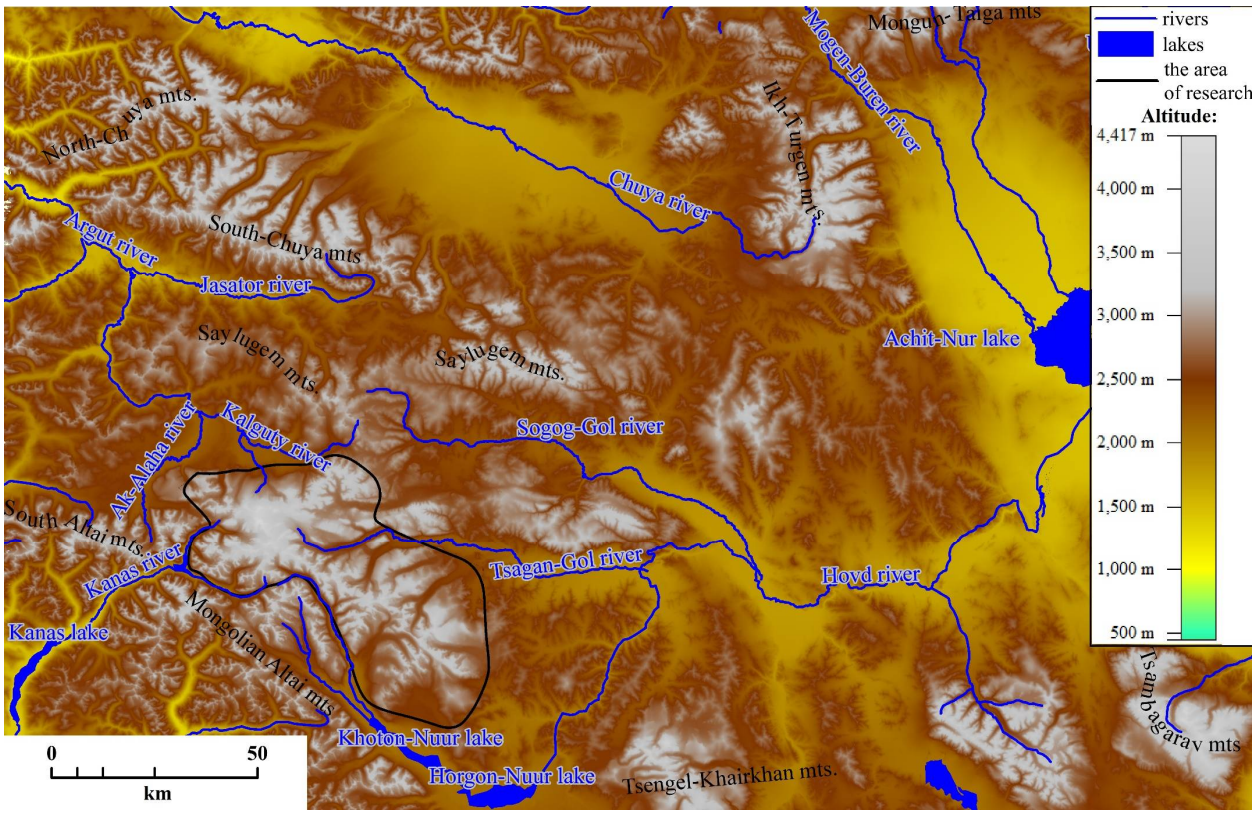

Fig. 1. Geographical location of the Tavan Bogd mountain range

Climate of the massif is determined by the Asian anticyclone in the winter. In the summer, when most of the annual precipitation falls, the cyclones that develop on the polar front prevail [28], the frequency of south-western (Aral, Caspian, and to a lesser extent Black Sea) cyclones is great, which strongly influences the formation of precipitation. The western part of the massif that is not shielded from the western streams is accessible for penetration from the west (through the valley of the Bukhtarma River) and especially from the southwest (through the valley of the Kanas River). Climatic conditions are best known for the northern slope. The closest (only 10 km from the glaciers) meteorological station Bertek (altitude 2200 m a.s.l.) was functioning between 1959 and 1982. According to the data of the weather station, the climatic conditions at the foot of the massif are characterized by low temperatures (average summer temperature 8.2 °C, average annual temperature -8.3°C). Precipitation is low (average annual precipitation 200.6 mm) with a pronounced summer maximum (59% of the annual total precipitation) and almost snowless winter (5% of the total). In the glaciated zone annual precipitation is sufficiently higher, for example on the firn line altitude it increases from about 365 mm to 880 mm from the east to the west along the slope [29].

Climatic conditions of the western and south-western slopes are less known. The closest meteorological stations are situated in Kazakhstan – Orlovskiy village (1106 m. a.s.l.) and Katon-Karagai (1081 m. a.s.l.), about 90 km to the south-west and 140 km to the west of the nearest glaciers of Tavan Bogd, respectively. In China the nearest weather stations are Habane (534 m a.s.l.) and Altai (736.9 m. a.s.l.) about 140 and 120 km to the south-west of the glaciers. Precipitation is higher than on the northern slope (354 mm in Orlovskiy village and 457 mm in Katon-Karagai) with less pronounced summer maximum (41-42% of the annual precipitation) and winter minimum (18-12 %). According to the snow pit data from the Kanas glacier (south-western slope), the annual precipitation at the ELA is 700-800 mm water equivalent [30–32].

Glaciers of the north-eastern slope of Tavan Bogd are located about 100 km from the nearest meteorological stations: Ulgi (1716 m a.s.l.) in the east and Altai (2182 m a.s.l.) in the south-east. Climatic conditions are sufficienty drier, for example, in Ulgi average annual precipitation is only 128.5 mm. 67% of this amount comes in the summer months, only 2% in the winter months. Climatic conditions in the glaciated zone have been estimated by in situ measurements made by automatic station at altitude 3040 m a.s.l. In 2007 summer season precipitation was 191.6 mm, which is sufficiently higher than Ulgi (54.2 mm for the same period)[33]. With such pluviometric gradient (10mm/100 m) used for the annual precipitation its value for the ELA can be estimated about 300 mm. Other estimations, based on the results of modelling without direct observations give higher values: 785 mm [34], 790 mm [35] and even 1000 mm [36].

The glaciers of Tavan Bogd were first discovered in 1897 by V.V. Sapozhnikov [37]. In 1905 he opened the largest glacier in the Altai-Sayan mountain region - the Potanin Glacier. From 1905 to 1909, he studied and mapped all the main glaciers of the massif. In 1916 B.V Tronov and M.V. Tronov visited the Przhevalsky (Halasi) and Potanin glaciers before climbing to the summit of Kiytyn [38]. In the Catalog of the Glaciers of Altai in 1925 Tavan Bogd was represented by 36 glaciers with a total area of 158 km2 [39]. The massif was kept away from glaciological research up to 1959, when Chinese glaciologists started the study of glaciers in the upper reaches of the river Khalasi (Kanas), as a result the glaciers of the Chinese part of Tavan Bogd were included into the Glacier Inventory of China [30,32].

In 1964 glaciological studies of the northern slope of Tavan Bogd were started by the scientists of Tomsk University for the collection of data in the compilation of the Catalog of Glaciers of the USSR [40,41]. In 1984 they were continued by carrying out geodetical surveys of the largest glaciers [42]. In 1971 Selivanov and Bjamba [43] on the basis of aerial imagery estimated the area of snow-firn fields of the Mongolian part of Tavan Boghd by 94 km^2 [43]. In 1987 several glaciers of Tavan Bogd including 2 glaciers on the northern slope and Potanin glaciers were studied by the Soviet-Mongolian glaciological expedition. Basing on those results the total area of the glaciation of Tavan Bogd in 1987 was estimated by 222.3 km^2, also a rough estimate of the LIA area of the glaciers has been made (260 km^2)[44]. Since 1999 the glaciers of the north slope are continuously studied by the scientists of Saint-Petersburg state university (field observations and remote sensing)[45–48]. In 2000-2001 a group of scientists from the Altai State University made field observations of the glaciers of the northern slope and of the largest Mongolian glaciers of Tavan Bogd [49]. In 2001 Galakhov and R'edkin estimated the glaciation of the Mongolian part of the massif by about 134 km^2. In 2005-2009 mass balance and geophysical studies of Potanin glacier were held by Japanese-Mongolian group of scientists [33,50–52] . Since 2013 the scientists of Saint-Petersburg State University make field observations of Potanin and Kozlov glaciers in Mongolia [34].

In recent years, significant progress has been made in the study of the glaciers of Tavan Bogd due to the use of remote methods [53,54], in particular in the compilation of the second Chinese glacier Inventory [55] and GLIMS (Global Land Ice Measurements from Space) database and the Randolph Glacier Inventory [56].

However, the information about present and past glaciation of Tavan Bogd is far from being full. First, the data about the recent glaciation are fragmentary (mostly due to studies confined by borders of different First, the data on modern glaciation are fragmentary, mainly due to research

within the borders of individual states. Consequently, these data were obtained from different materials, by different methods, with varying accuracy, and refer to different years. At the same time, the results of field observations are to a small extent involved. Second, there is almost no information about the glacial extent during the LIA. Third, the information about the glacial recession is also fragmentary and refers mostly to the period after 1990.

Accordingly, the aims of this article are the following:

1. To give a full description of the scale and structure of modern glaciation

2. To reconstruct the glaciation in the Little Ice Age

3. To estimate the extent of the glaciers in 1968

4. To determine the main trends of the change in glaciation from the maximum of the LIA and their causes

2. Materials and methods

This article is mostly based on the results of studies that include 3 groups of methods.

2.1. Continuous monitoring observations of the glaciers.

Since the late 1980-s the geographers of Saint-Petersburg (our research group) established the monitoring of the glaciation of Altai mountains in the regime of part-time observation stations (hydrological, glaciological (mass balance, firn line altitude, retreat from the benchmarks etc.), meteorological, geomorphologic, dendrochronological, in situ observations were made in the ablation periods).

Since 1999 such field study is done for Tavan Bogd massif. Expeditions took place in 1999, 2000, 2001, 2002, 2003, 2004, 2006, 2009, 2011, 2013, 2014, 2015, 2018, mostly to the northern (Russian) part of the massif. Glaciological observations included monitoring of the positions of the glacial edges, locating the ELA, mass balance observations and mass balance index calculations. Monitoring of the positions of the glacial edges is based on survey activities, such as geodetic surveying, GPS-trekking of the glacial edges, measurements of the changes of the glacial length (repeated measurements of the distance between the benchmarks and the glacial edges), the usage of repeated photographs and remote sensing. The results of such monitoring give the opportunity to estimate the rates of advance and retreat of the glaciers.

The monitoring of the positions of the glacial edges was done for different types of the glaciers, but preference was given to the larger valley glaciers that are the most representative glaciers (due to less dependence of geomorphic factors) with the longest observation periods (being at the same time easier to reach due to lower positions of the snouts). The largest valley glaciers Argamgi-3 and Argamgi-2, have the longest in situ observation range starting from 1984. There are also nine glaciers (two cirque, one corrie-valley, six slope glaciers) where the continuous instrumental observations started from 2000-2001.

2.2. Remote sensing

Remote sensing study was based on the analysis of space imagery of the spatial resolution from 0.5 up to 80 meters per pixel collected on years 1968-2013 and aerial photos of 1962 (tab. 1). Most

of them were provided by RDC ScanEx (www.scanex.ru) and processed by the Space and Geoinformation Technologies Resource Center of Saint-Petersburg State University, several images were provided by the USGS (// (http://earthexplorer.usgs.gov)/).

The choice of time slices for the inventarization of glaciation was, in many respects, due to the availability of high-resolution satellite images necessary for this (Tab. 1). In addition to the high resolution of the image, they had to meet several more requirements: to correspond to the end of the ablation season, when the height of the snow line is maximal, and the snow cover does not interfere with delineation of the boundaries of glaciers; it is desirable to have no clouds; images should not be taken after snowfalls. High resolution SPOT-5 and Geoeye-1 images taken in 2010 covered over 90% of the glaciated area of Tavan Bogd, excluding the far eastern periphery. Consequently, 2010 was chosen as a suitable year for the characteristic of recent glaciation of Tavan Bogd. For the eastern periphery of the glaciated area Landsat-5 imagery was used. The second time slice refers to 1968: we made the reconstruction of the glaciation on the basis of Corona satellite images.

Other satellite and aerial imagery (2013, 2008, 2007, 2006, 1989, 1977, 1962) were used to get additional information for several largest glaciers.

Tab. 1. Satellite and aerial imagery used in the study of Tavan Bogd glaciers.

Satellite and aerial imagery			
Scene ID	Date	Spacecraft	Spatial resolution, m
LC81440262018213LGN00	2018-08-01	LANDSAT_8	15
LC81430262018190LGN00	2018-07-09	LANDSAT_8	15
SP5_216251_1308220445377_1A_1T	2013/08/22	SPOT 5	2.5
LT51430262010216IKR00	2010/08/04	LANDSAT_5	30
LT51430262010232IKR00	2010/08/20	LANDSAT_5	30
LT51440262010239IKR00	2010/08/27	LANDSAT_5	30
LT51430262010264IKR02	2010/09/21	LANDSAT_5	30
o_731905 (0000016-0000021)	2010/07/24	Geoeye-1	0.5
SP5_214251_100831_itog	2010/08/31	SPOT 5	2.5
P5_550174_20080727_	2008/07/27	Cartosat-1	2.5
P5_547173_20080716	2008/07/16	Cartosat-1	2.5
S2S1L0_215251_070912	2007/09/12	SPOT 2	20
S2P1L0_215251_060723	2006/07/23	SPOT 2	10

Preprints (www.preprints.org) | NOT PEER-REVIEWED | Posted: 18 August 2018 doi:10.20944/preprints201808.0332.v1

Peer-reviewed version available at Geosciences 2018, 8, 414; doi:10.3390/geosciences8110414

S2P2L0_215251_060601	2006/06/01	SPOT 2	10
LE71440262000220SGS00	2000/08/07	LANDSAT_7	15-30 m
LE71430262000229SGS00	2000/08/16	LANDSAT_7	15-30 m
LT51430261998247BIK00	1998/09/04	LANDSAT_5	30 m
LT51440261998238BIK00	1998/08/26	LANDSAT_5	30 m
LT51430261998215BJC00	1998/08/03	LANDSAT_5	30 m
LM51440261989229ISP01	1989/08/17	LANDSAT_5	80
LM21550261977209AAA03	1977/07/28	LANDSAT_5	80
DS1104-1039DA010-013	1968/08/10	CORONA	1.8
M-45-103, M-45-104	1962/08/24	Aerial	

Every scene was radiometrically normalized and geographically referenced using orbital parameters. The automatic systematic geometric correction of raster data was applied, that based on mathematical model of the view angles of satellite camera and its position at the moment of the scene collection (rigorous model). UTM/WGS 84 projection (zone 46) has been identified as the reference frame for the georeferencing. The imagery has been orthorectified using 30 m SRTM 1 Arc-Second Global (DEM) downloaded from the USGS EROS Data Center (www. https://eros.usgs.gov/) and treated with moderate-sharpening filter for graphic quality preservation.

All aerial photographs were also geographically referenced using ground control points (GCP) and transformed into the international coordinate system (UTM /WGS 84, zone 46).

Processing of space imagery and aerial photographs was carried out using photogrammetric software.

The mapping of glaciers was done manually; the minimum size of glaciers to be mapped was 0.01 km^2. To determine the accuracy of the manual interpretation of the boundaries of the glaciers, the repeated contouring of several glaciers with an area of more than 0.1 km^2 has been done. As a result, it was revealed that the error in determining the area of individual glaciers is less than 5%. The error in determining the area of a large sample of glaciers (more than 100) is reduced to <3% by compensating for positive and negative errors. SRTM 30 m DEM was used to outline the ice divides in areas with continuous glacial cover.

In the areas where no field observations were held the boundary line between the glacier and the dead ice was found using indicators defined by Loibl et. al. [25]: active ice indicators are “smooth” debris surface, linear flow structures, constrained tributaries; dead ice indicators are rugged debris surface, melting ponds, unconstrained tributaries, pioneer plants. We should also add another typical feature of dead ice- the water flow into the tunnels and their exit from other tunnels down the slope. All those indicators work well with the only exception of pioneer plants, which due to

dry climate are absent near the glaciers and appear only on the surface of inactive rock glaciers. In our area of research, it is typical when the active glacial edge is marked by marginal flows that join at the lowest point of the glacier.

Other typical problems are overestimating of the glacial area after the snowfalls or when the seasonal snow cover has not melted down yet and the shading of some parts of the glacier and the adjacent non-glacial areas. The ways to solve those problems are: to use images made in the end of ablation season and with least snowiness and to compare the images of the same area with different acquisition time and different sun angle.

We used a 30 m SRTM 1 Arc-Second Global (DEM) USGS EROS Data Center (www. https://eros.usgs.gov/) to characterize our glacier outlines with parameters including: mean, minimum, and elevation ranges, mean slope and mean aspect.

The present firn line altitude in the area of research is generally equivalent of ELA (the difference is usually within 10 m). The firn line altitude was found by combination of direct observations and analysis of satellite imagery. We used images with acquisition dates at the end of the ablation seasons.

On some small glaciers the firn line was not distinguished, in those cases Kurowsky method [57,58] was used. In this method the firn line altitude or ELA is calculated as the average altitude of the glacier: $\overline{z}_f = \sum_i \frac{f_i z_i}{F}$, where $\overline{z}_f$ - firn line altitude or ELA, f_i - areas of different altitudinal zones of the glacier, z_i - average altitudes of these zones, $F = \sum_i f_i$. The calculations were based on the measurements from the topographic maps (1:100000, 1:50000 for Tavan Bogd, 1:25000 for Mongun-Taiga). Kurowsky method was also used to verify the values of ELA, found by remote sensing.

2.3. Paleo reconstructions.

Reconstruction of the LIA extent of the glaciers was done on the basis of geomorphological methods. LIA moraines were mapped using space imagery, aerial photos, tachometry, GPS-tracking of the lateral and terminal moraines, visual in situ observations. We used the method of ground-based route interpretation that included descriptions, measurements and photography in reference areas. The measurements in the mountain massif were all made by using GPS (USA). Recognition of objects used the method of visual interpretation according to reference standards [59,60]. They were compiled from ground-based observations, indicating the following characteristics: characteristic images of objects on the terrain, on the aerial photograph, on the satellite image and on the topographic map; distinctive characteristics of objects, and methods of transferring objects to the map. The criteria which we used to identify moraines using the satellite imagery and DEM are largely similar to those suggested in [61]: “identification criteria include shadowing due to changes in topography (relative relief) and changes in color due to changes in soil, soil moisture, and vegetation cover. Associated landforms such as deflected abandoned meltwater channels are also useful in delineating the break-of-slope of these features.” Furthermore, we used high-resolution images and compared interpretation results with in situ field observations. Recently the same study has been done for Mongun-Taiga mountain massif (Russian

Altai), having some similar features of present and past glaciation and its climatic conditions [62], this experience also was useful.

A characteristic property of the study area favorable to visual interpretation includes the long-lasting persistence of glacial topographic features, and the inheritance of the links between the formations of glacial genesis associated with climate aridity, low erosion rates, low rates of biological processes and poor development of land cover. Low temperatures, high intensity of frost weathering and small precipitation amounts promote a long-lasting preservation of buried glacier ice. All this serves as the cause for the sharpness of most glacial landforms on aerial photographs and satellite images whose interpretation is eased by an almost total absence of forest vegetation.

Diagnostic features of LIA moraines are their bareness, steep fronts and relatively big thickness, glacial ice cores that are sometimes exposed by thermokarst processes, position adjacent to modern glaciers. The low turfness of LIA moraines (Fig. 2) in multispectral images is expressed by grey or brown color of moraines, in sharp contrast with greenish color of the surrounding subalpine meadows and tundras so that are easily identified. This is particularly characteristic for the moraines from the Little Ice Age which, usually, partly or fully overlap the more ancient moraines of the historical stage. The third characteristic feature is the presence of the ice core of glacial origin. Starting in the late 1990s, an intensification of thermokarsting processes on the moraines from the Little Ice Age has given rise to numerous thermokarst depressions, thermoerosional forms and landslides [6], standing out in steep areas of dumped moraines in the form of sharp and contrasting dark bands visible on images with a resolution better than 15 m.

Preprints (www.preprints.org) | NOT PEER-REVIEWED | Posted: 18 August 2018 doi:10.20944/preprints201808.0332.v1

Peer-reviewed version available at Geosciences 2018, 8, 414; doi:10.3390/geosciences8110414

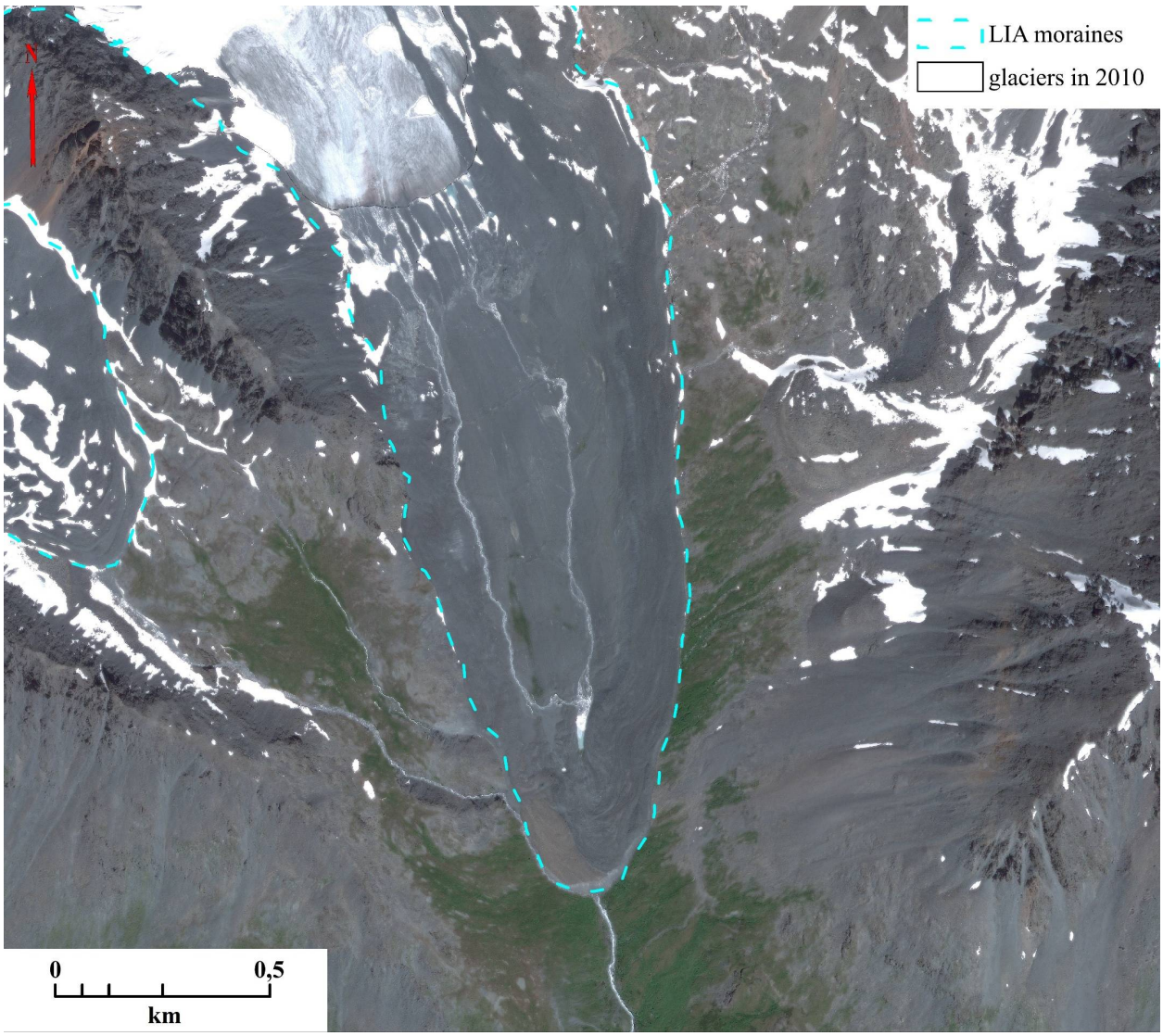

Fig. 2. Delineation of the LIA moraine, Postigiyn-Gol basin, using a Geoeye-1 image.

The end of the LIA maximum and the start of the general retreat of the glaciers was referred to 1810-1820, basing on our studies in the neighboring areas of the Russian Altai [27].

3. Results

Recent glaciation.

According to our studies the glaciation of Tavan Bogd in 2010 was represented by225 glaciers with total area about 201 km^2 (tab. 2, fig. 3). The lowest point altitude was 2496 m, the maximal is 4374 m (Khuiten Uul pek). The weighted average ELA was 3285 m.

Tab.2. Glacier inventory of Tavan Bogd for 2010.

№	L	H1	H2	M	S	ELA	a	A1	A2	River Basin
1	0.18	3330	3433	hanging	0.01	3395	31	0	0	Kalguty
2	0.51	3182	3460	hanging	0.08	3420	29	10	10	
3	0.36	3232	3480	hanging	0.02	3385	35	12	12	
4	0.53	3229	3503	cirque	0.21	3395	28	28	28	
5	0.53	3133	3448	hanging	0.06	3300	31	2	2	
6	0.57	3200	3511	hanging	0.05	3355	29	355	355	
7	0.59	3187	3471	hanging	0.10	3355	26	359	359	
8	0.41	3209	3338	cirque	0.10	3300	18	328	328	
9	0.23	3302	3452	hanging	0.02	3415	33	14	14	
10	0.91	3150	3520	cirque	0.38	3425	22	34	0	
11	1.17	3330	3601	slope	0.68	3505	14	306	0	
12	1.33	3232	3550	cirque	0.82	3405	15	20	0	
13	2.56	3107	3970	slope	2.76	3425	19	30	30	
14	2.30	3093	4012	slope	2.07	3325	21	16	6	
15	1.32	3328	3885	hanging	0.26	3420	24	345	12	
16	2.72	3011	3902	slope	1.52	3565	18	45	26	
17	3.27	3115	4093	slope	2.75	3380	18	49	30	
18	2.31	3066	4103	slope	1.46	3320	24	359	4	
19	1.87	3208	4096	slope	0.75	3430	26	336	0	
20	3.92	3050	4083	valley	4.77	3380	19	309	12	
21	0.52	3466	3866	hanging	0.21	3695	38	76	80	
22	0.99	3331	3868	hanging	0.32	3595	30	356	328	
23	2.57	2860	3710	valley	3.32	3110	18	20	3	

Preprints (www.preprints.org) | NOT PEER-REVIEWED | Posted: 18 August 2018 doi:10.20944/preprints201808.0332.v1

Peer-reviewed version available at Geosciences 2018, 8, 414; doi:10.3390/geosciences8110414

24	0.32	2981	3089	niche	0.05	3350	19	10	10	
25	0.36	3187	3325	cirque-hanging	0.11	3225	21	19	356	
26	2.12	2852	3487	cirque-valley	1.37	3115	25	20	325	
27	0.51	2935	3236	hanging	0.04	3100	31	11	353	
28	0.20	3158	3253	hanging	0.01	3225	28	296	338	
29	0.64	2850	3161	cirque-hanging	0.12	2980	28	21	353	
30	0.83	2989	3327	cirque	0.35	3110	23	336	279	Ak-Alaha
31	1.10	2905	3324	cirque	0.51	3045	23	12	345	
32	1.49	3135	3489	slope	0.73	3425	15	242	297	
33	0.42	3405	3469	slope	0.06	3450	8	138	161	Sangadyr
34	1.06	3051	3385	cirque	0.34	3140	18	290	281	
35	1.18	2983	3419	cirque	0.34	3145	21	288	278	
36	2.41	2805	3668	cirque-valley	2.52	3250	27	4	272	
37	1.79	3272	3667	slope	0.48	3450	15	233	187	
38	6.30	2932	4093	valley	10.29	3300	15	287	214	
39	1.39	3170	3441	cirque-valley	0.58	3250	11	232	204	
40	3.49	3102	4280	valley	1.38	3335	24	212	185	
41	0.28	3086	4043	hanging	0.02	3925	41	301	301	
42	0.62	3684	4129	hanging	0.17	3905	36	254	272	
43	0.25	3640	3828	hanging	0.01	3776	39	244	206	
44	0.15	3790	3895	hanging	0.01	3825	33	254	221	
45	0.54	3279	3625	niche	0.11	3375	35	264	239	
46	9.61	2496	4318	valley	24.49	3175	15	323	305	

47	1.31	3290	3898	cirque-valley	0.31	3390	26	260	257	
48	2.07	2978	3713	valley	0.87	3205	21	271	285	
49	1.10	2970	3835	cirque	0.50	3345	40	3	334	
50	0.39	3457	3940	hanging	0.04	3710	52	357	22	
51	0.49	3134	3626	hanging	0.05	3440	48	341	22	
52	0.21	3336	3537	hanging	0.01	3435	45	17	29	
53	0.33	3167	3340	hanging	0.03	3270	27	358	346	
54	0.45	3606	3932	cirque-hanging	0.04	3770	37	302	296	
55	1.22	3170	2936	cirque	0.32	3460	33	282	267	
56	5.95	2661	3701	valley	8.75	3135	11	354	297	
57	1.42	2810	3444	valley	0.52	3015	28	11	67	
58	0.60	2793	3290	cirque	0.10	3050	28	30	60	
59	1.24	2830	3500	cirque-valley	0.38	3275	32	12	317	
60	0.23	3114	3362	hanging	0.01	3255	47	359	8	
61	1.63	2831	3486	valley	0.73	3170	24	0	309	
62	0.63	2978	3483	hanging	0.13	3230	39	9	9	
63	0.76	2955	3420	cirque-valley	0.27	3235	32	338	314	
64	2.96	2810	3580	valley	1.83	3160	16	330	288	
65	0.35	3040	3278	hanging	0.04	3240	35	59	23	
66	0.18	3297	3400	hanging	0.01	0	30	35	35	
67	0.35	3085	3433	hanging	0.01	3290	46	1	35	
68	1.05	2792	3259	cirque	0.16	2895	24	318	324	
69	0.48	2994	3273	cirque-hanging	0.14	3165	35	287	353	
70	0.30	3104	3242	hanging	0.03	3205	24	27	27	

Preprints (www.preprints.org) | NOT PEER-REVIEWED | Posted: 18 August 2018 doi:10.20944/preprints201808.0332.v1

Peer-reviewed version available at Geosciences 2018, 8, 414; doi:10.3390/geosciences8110414

71	2.05	2951	3587	valley	0.91	3200	25	347	31	
72	0.32	3191	3454	cirque	0.04	3310	40	310	303	
73	1.11	3097	3500	cirque	0.33	3225	21	75	109	
74	1.17	2993	3409	cirque	0.43	3130	20	289	264	
75	0.34	3300	3463	slope	0.20	3410	27	207	191	
76	1.25	2911	3483	cirque	0.70	3100	13	345	269	
77	0.45	2812	3072	niche	0.14	2915	30	327	311	
78	1.02	2871	3230	cirque	0.33	3025	26	13	291	
79	1.34	2940	3388	cirque-valley	0.60	3050	19	93	82	Budiuhanasıhe
80	0.62	3071	3342	cirque	0.16	3125	26	206	158	
81	1.84	3041	3463	valley	1.02	3200	16	295	225	
82	2.02	3018	3553	valley	1.42	3200	16	142	128	
83	2.24	3020	3670	valley	2.12	3230	18	195	152	
84	2.96	2967	3750	valley	1.41	3210	17	239	180	
85	0.75	3089	3432	cirque	0.25	3165	27	159	117	
86	2.5	2983	3765	valley	1.15	3285	20	190	169	
87	4.15	2799	3753	valley	5.59	3150	10	226	222	
88	0.48	2977	3265	niche	0.06	3120	31	279	311	
89	1.1	2872	3316	niche	0.80	2960	23	344	339	
90	0.71	2811	3195	cirque	0.32	2930	29	359	348	
91	1.32	3051	3398	niche	0.60	3135	17	138	197	
92	2	3015	3400	cirque-valley	1.32	3175	11	145	132	Postigiyn- Gol
93	0.18	3100	3230	slope	0.02	3200	36	27	27	
94	0.85	2839	3196	cirque-valley	0.23	2925	24	24	38	
95	0.07	3400	3434	slope	0.01	3415	17	61	61	

Preprints (www.preprints.org) | NOT PEER-REVIEWED | Posted: 18 August 2018 doi:10.20944/preprints201808.0332.v1

Peer-reviewed version available at Geosciences 2018, 8, 414; doi:10.3390/geosciences8110414

96	0.4	3177	3407	cirque	0.05	3270	30	73	83	
97	0.98	2843	3428	cirque	0.30	3290	31	358	66	
98	3.23	2840	3565	valley	5.17	3165	11	95	81	
99	1.8	2956	3614	cirque	1.10	3100	20	61	63	
100	6.76	2674	3935	valley	9.70	3235	12	146	166	
101	0.35	3360	3515	slope	0.03	3290	25	172	143	
102	0.53	3133	3306	cirque	0.19	3200	18	110	110	
103	3.08	3069	3767	valley	2.64	3310	14	183	135	
104	0.58	3258	3383	niche	0.11	3315	13	182	148	
105	0.59	3521	3658	slope	0.07	3620	14	223	183	
106	0.6	3528	3743	hanging	0.39	3665	20	212	208	
107	1.68	3045	3590	cirque-valley	1.00	3180	19	106	148	
108	0.4	3207	3369	hanging	0.06	3310	28	343	319	
109	0.08	3467	3480	flat summit	0.01	3475	3	232	232	
110	0.2	3285	3406	hanging	0.02	3330	31	91	81	
111	0.09	3433	3464	slope	0.01	3450	19	87	87	
112А	1.14	3282	3603	slope	0.54	3445	16	292	272	
113	0.23	3213	3293	hanging	0.02	3265	20	66	66	
114	0.3	3262	3306	slope	0.03	3285	8	301	305	
115	0.16	3252	3285	slope	0.02	3270	10	38	69	
112Б	0.22	3524	3602	slope	0.09	3565	20	148	148	
116	1.08	3034	3391	cirque	0.37	3100	13	60	95	
117	0.76	3137	3441	cirque	0.33	3320	27	47	95	
118	0.51	3442	3563	flat summit	0.29	3455	11	146	151	
119А	2.24	3183	3484	flat summit	1.53	3455	8	273	304	
120	0.18	3144	3240	slope	0.04	3200	26	338	338	

Preprints (www.preprints.org) | NOT PEER-REVIEWED | Posted: 18 August 2018 doi:10.20944/preprints201808.0332.v1

Peer-reviewed version available at Geosciences 2018, 8, 414; doi:10.3390/geosciences8110414

121	0.23	3115	3263	slope	0.09	3205	33	346	346	
122	0.32	3156	3311	hanging	0.05	3235	26	317	341	
123	0.29	3185	3287	slope	0.04	3265	20	309	309	
124	0.59	3136	3466	cirque-hanging	0.14	3290	30	338	321	
125	0.29	3168	3405	hanging	0.03	3305	43	317	359	
126	0.29	3163	3386	hanging	0.04	3310	37	355	355	
127	0.21	3251	3394	hanging	0.02	3385	37	25	346	
128	0.21	3213	3391	hanging	0.02	3355	41	341	358	
129	0.38	3094	3307	hanging	0.07	3280	30	10	4	
130	0.49	2977	3114	hanging	0.06	3055	16	358	342	
131	0.44	3370	3455	slope	0.06	3435	11	261	314	
132	0.97	3002	3361	cirque-hanging	0.19	3210	23	43	355	
133	0.23	3339	3371	slope	0.03	3355	8	62	106	
134	0.19	3422	3444	slope	0.01	3440	7	191	154	Arshan-Gol
135	0.48	3238	3457	slope	0.08	3440	26	50	47	
136	1.23	3016	3475	cirque-valley	0.35	3265	21	25	29	
137	0.31	3222	3360	slope	0.04	3295	22	7	32	
138	1.14	3133	3493	cirque-valley	0.40	3245	21	25	58	
139	0.68	3098	3453	cirque	0.34	3265	30	40	76	Mogotiyn-Gol
140	0.28	3292	3384	slope	0.04	3330	19	83	113	
141	0.55	3405	3584	slope	0.47	3485	13	47	69	
142	0.73	3043	3485	cirque-hanging	0.27	3285	33	25	336	
143	0.67	3263	3456	cirque-hanging	0.12	3350	15	22	53	

144	0.35	3202	3497	cirque-hanging	0.08	3370	41	353	350	
145	0.66	3258	3508	cirque	0.29	3390	21	22	29	
146	0.17	3460	3558	slope	0.11	3500	24	18	18	Ikh-Hatugiyn Gol
147	0.77	3103	3533	cirque	0.45	3405	29	24	24	
148	0.13	3260	3389	hanging	0.03	3340	31	342	8	
149	0.57	3064	3409	cirque	0.14	3185	32	18	52	
150	0.24	3299	3465	cirque-hanging	0.01	3440	35	17	17	
151	0.5	2959	3165	cirque	0.08	3035	23	41	350	
152	0.34	3108	3384	hanging	0.04	3350	39	350	11	
153	0.38	3122	3396	hanging	0.05	3355	37	15	15	
154	0.33	3162	3409	hanging	0.04	3340	37	10	359	
155	0.61	3096	3426	cirque	0.22	3260	29	346	22	
156	1.72	3161	3567	cirque-valley	0.94	3345	13	21	48	
157	0.2	3257	3391	hanging	0.02	3350	34	334	358	Baga-Hatugiyn Gol
158	0.52	3163	3429	cirque	0.14	3255	25	0	24	
159	0.43	3452	3660	cirque-hanging	0.07	3535	27	56	39	
160	1.52	3033	3660	valley	0.60	3310	23	337	0	Nalia-Gol
161	1.91	3002	3627	valley	1.42	3220	20	6	359	
119B	1.7	3286	3484	flat summit	1.14	3455	7	342	315	
162	0.2	3228	3380	slope	0.06	3345	30	81	81	
163	0.12	3252	3358	slope	0.03	3295	15	36	36	
164	0.26	3044	3220	hanging	0.02	3140	35	38	38	
165	0.28	3084	3272	hanging	0.01	3225	34	343	328	
166	0.59	2930	3276	cirque-hanging	0.11	3160	31	0	0	

Preprints (www.preprints.org) | NOT PEER-REVIEWED | Posted: 18 August 2018 doi:10.20944/preprints201808.0332.v1

Peer-reviewed version available at Geosciences 2018, 8, 414; doi:10.3390/geosciences8110414

167	0.75	2907	3177	cirque	0.10	3020	21	54	49	
168	0.18	2942	3043	cirque-hanging	0.02	3010	30	18	18	
169	0.19	3044	3140	cirque-hanging	0.01	3070	0.19	64	64	
170	0.44	2943	3278	hanging	0.02	3140	38	0	0	
171	0.56	3223	3479	cirque	0.20	3370	23	10	26	
172	1.19	2957	3523	cirque-valley	0.33	3170	27	36	46	
173	0.17	3353	3508	hanging	0.02	3480	47	4	76	
174	1.36	3031	3436	valley	0.49	3280	18	35	29	
175	0.27	3359	3498	hanging	0.05	3430	27	112	93	
176	1.41	3110	3527	valley	0.95	3275	18	13	65	
177	0.58	3121	3359	cirque	0.17	3365	26	20	28	Tsagan-Gol
178	2.15	3043	3588	valley	1.47	3395	15	0	0	
179	0.61	3404	3550	slope	0.24	3435	14	61	50	
180	0.73	3082	3228	cirque-valley	0.18	3230	28	45	1	
181	1.65	2910	3576	valley	1.31	3105	24	6	340	
182	0.75	2852	3257	cirque	0.33	2980	27	8	12	
183	1.33	2971	3445	cirque-valley	0.74	3120	24	26	72	
184	1.78	2973	3357	valley	0.71	3130	13	88	50	
185	0.52	3044	3315	cirque	0.14	3210	30	19	67	
186	0.16	3198	3300	hanging	0.01	3285	20	304	300	
187	0.23	3150	3302	hanging	0.02	3280	34	339	339	
188	2.34	2818	3354	valley	1.14	3060	13	4	7	
189	1.8	3001	3533	cirque-valley	0.95	3150	18	27	64	

190	0.41	3046	3199	niche	0.07	3125	20	81	59	
191	0.35	3218	3295	niche	0.04	3255	13	75	60	
192	0.32	3144	3296	cirque	0.05	3170	26	302	301	
193	4.66	2861	3779	valley	4.74	3150	12	28	36	
194	0.74	3182	3493	cirque	0.23	3275	23	73	72	
195	6.08	2809	3934	valley	9.55	3320	10	66	84	
196	0.62	3433	3880	hanging	0.03	3720	37	288	301	
197	1.22	3301	3959	hanging	0.39	3350	30	113	148	
198	1.22	3228	3603	cirque-valley	0.39	3375	17	47	70	
199	2.29	3055	3767	cirque-valley	0.92	3290	18	12	60	
200	0.31	3374	3654	hanging	0.03	3575	43	8	27	
201	0.38	3305	3595	hanging	0.04	3470	38	30	30	
202	0.37	3407	3691	hanging	0.05	3595	38	320	320	
203	8.88	2895	3971	valley	13.21	3395	6	50	86	
204	1.53	3198	3859	hanging	0.63	3455	24	57	39	
205	11.3	2911	4318	valley	23.63	3500	8	64	110	
206	0.1	3475	3544	hanging	0.01	3525	33	24	24	
207	0.09	3492	3560	cirque-hanging	0.01	3540	34	23	23	
208	0.4	3250	3528	cirque-hanging	0.08	3455	35	17	17	
209	0.79	3173	3594	cirque	0.13	3525	28	39	59	Ikh-Oygoryn-Gol
210	1.17	3238	3546	cirque	0.69	3400	16	18	77	
211	0.78	3323	3618	cirque	0.21	3555	21	91	78	
212	0.38	3329	3470	slope	0.04	3510	19	81	49	
213	0.38	3329	3470	slope	0.06	3410	19	81	49	

Preprints (www.preprints.org) | NOT PEER-REVIEWED | Posted: 18 August 2018 doi:10.20944/preprints201808.0332.v1

Peer-reviewed version available at Geosciences 2018, 8, 414; doi:10.3390/geosciences8110414

214	0.2	3246	3394	hanging	0.01	3340	36	5	5	
215	0.2	3284	3442	hanging	0.01	3405	39	67	32	
216	0.2	3320	3480	cirque-hanging	0.04	3455	35	53	54	
217	0.27	3317	3490	cirque-hanging	0.06	3460	31	55	40	
218	0.17	3412	3497	slope	0.03	3465	26	90	90	
219	0.19	3228	3490	slope	0.16	3370	17	76	69	
220	0.43	3065	3219	cirque	0.04	3115	22	51	113	
221	0.38	3306	3453	slope	0.09	3390	21	85	55	
222	0.28	3305	3437	slope	0.10	3410	22	53	18	
223	0.13	3253	3340	hanging	0.01	3315	34	17	45	
224	0.4	3064	3200	hanging	0.06	3130	19	50	50	Shepk-Oygoryn-Gol
225	0.33	3260	3410	cirque-hanging	0.12	3335	25	78	93	
					200.98					

L- maximal length, km; H1- the lowest point altitude, m; H2- the highest point altitude, m; M- morphologic type; S- area, km; ELA- average equilibrium line altitude, m; a- average slope angle, m; A1- average accumulation zone azimuth, ° ; A2- average ablation zone azimuth, °. Indices A, B after the same number of glaciers mean different slope aspects of parts of flat summit glaciers.

Preprints (www.preprints.org) | NOT PEER-REVIEWED | Posted: 18 August 2018 doi:10.20944/preprints201808.0332.v1

Peer-reviewed version available at Geosciences 2018, 8, 414; doi:10.3390/geosciences8110414

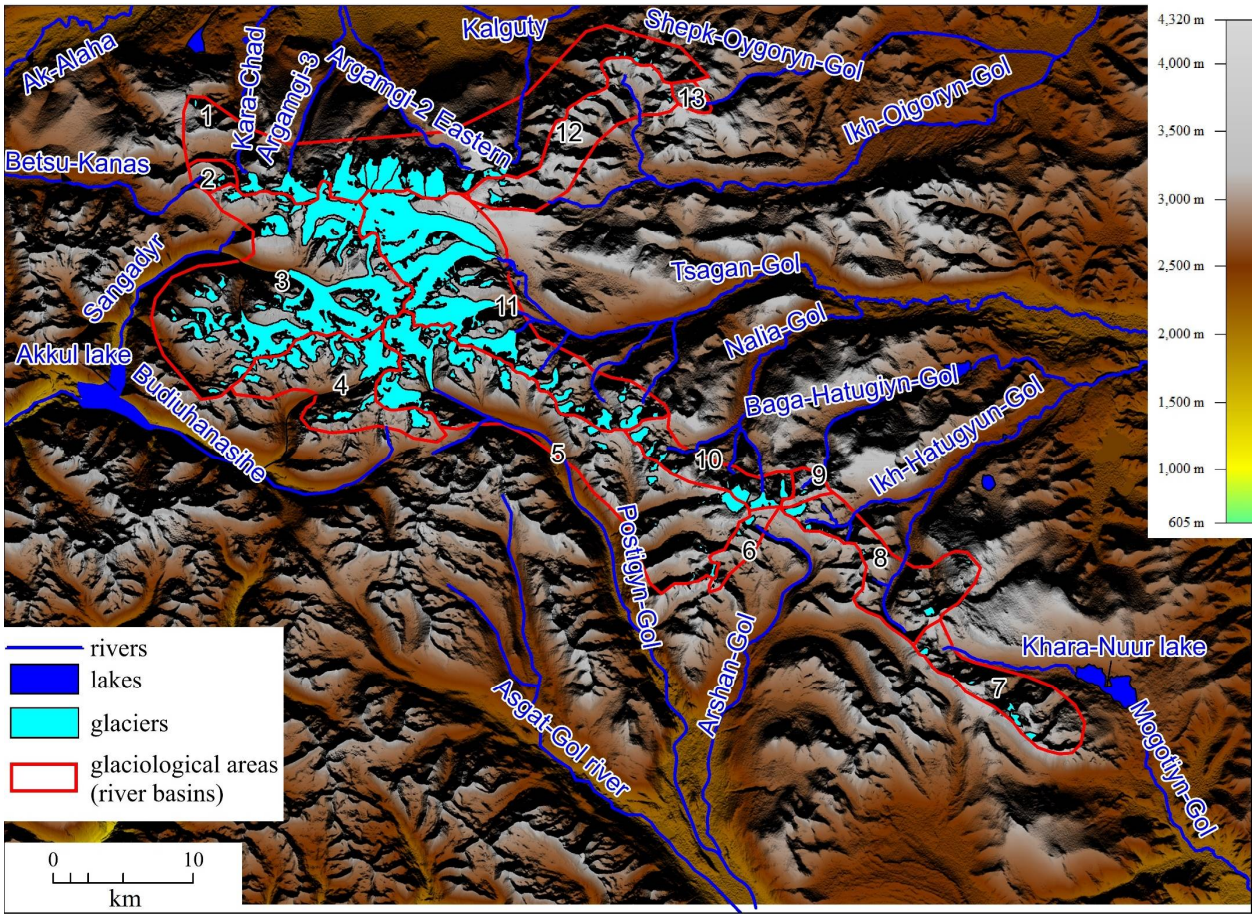

Fig. 3. Glacial areas (river basins) of Tavan Bogd. 1- Kalguty, 2- Ak-Alaha, 3- Sangadyr, 4- Budiuhansihe, 5- Postgiyn-Gol, 6- Arshan-Gol, 7- Mogotiyn-Gol, 8- Ikh-Hatugiyn-Gol, 9- Baga-Hatugiyn, 10- Nalia-Gol, 11- Tsagan-Gol, 12- Ikh-Oigoryn-Gol, 13- Shepk-Oygoryn-Gol

The distribution of the number of glaciers between the different area intervals has a clearly pronounced maximum in the range of less than 0.1 km. sq., and one more, secondary, in the range of 1.0-5.0 km^2. square (Figure 4). For the area, the contribution of the largest glaciers (more than 10 km^2) and glaciers in the 1-5 km^2 area is the most important. Obviously, it can be said that the largest compound valley glaciers (Potanin, Kanas) play the most important role in the glaciation of the massif, as well as the more numerous small (mainly simple) valley glaciers.

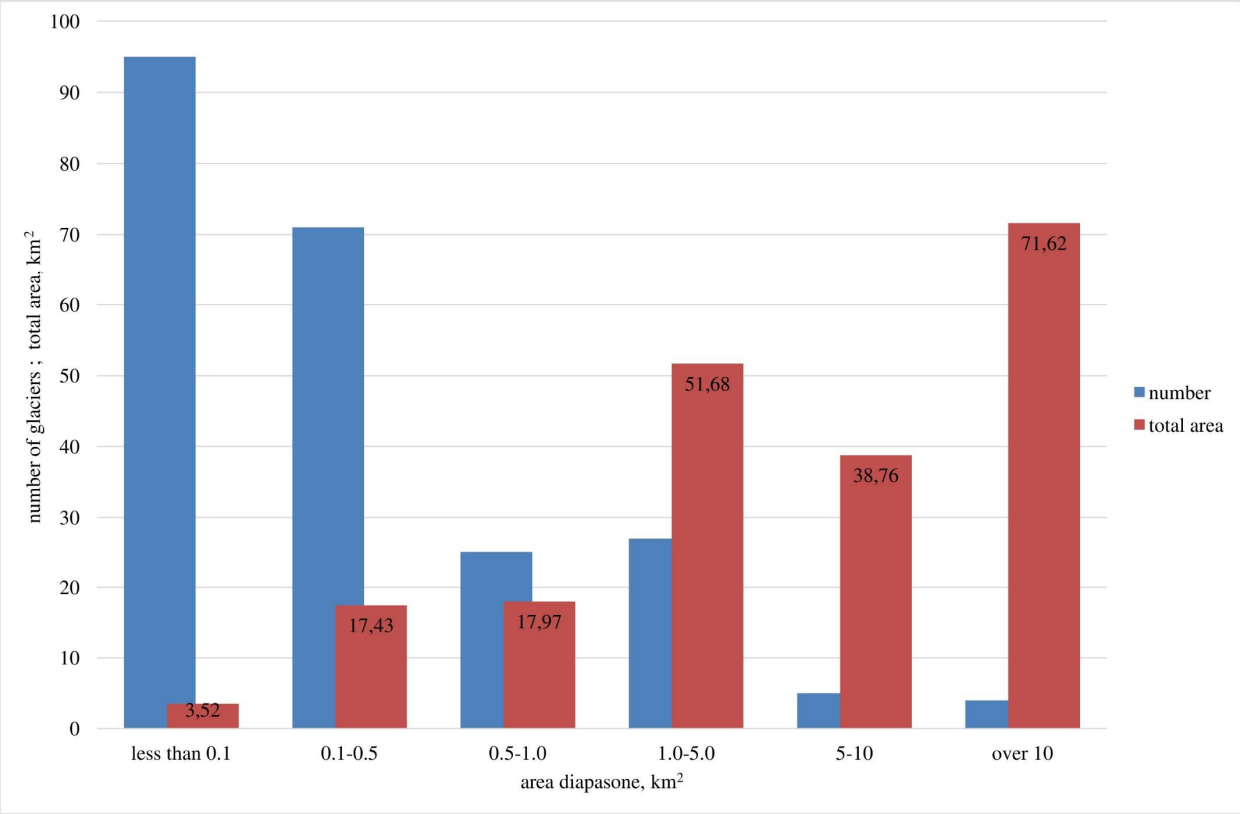

Fig. 4. Distribution of the quantity and total area of glaciers in different intervals of areas

The quantitative predominance of small glaciers and the area dominance of the largest glaciers is reflected in the distribution of glaciers along morphological types (Fig. 5, Fig. 6). The most common in the Tavan Bogd area are small hanging and cirque glaciers. At the same time, almost 3/4 of the total area of glaciation falls on the valley glaciers, which allows us to speak of Tavan Bogdo as a glacial center of the valley type. The relative development of large forms of glaciation manifests itself in comparison with the relative area of the valley glaciers of the nearest glacial centers (Ikh-Turgen ~50% [63], Mongun-Taiga~50% [64], Turgeni-Nuru ~55% [65], Kharkhiraa 58% [65]. Attention is drawn to the small number and area proportion of flat summit glaciers (1-2%), which is not typical for the Mongolian Altai and the southeast of the Russian Altai, for example in the total area of Tsambagarav ridge flat summit glaciers make about 40% [66] .

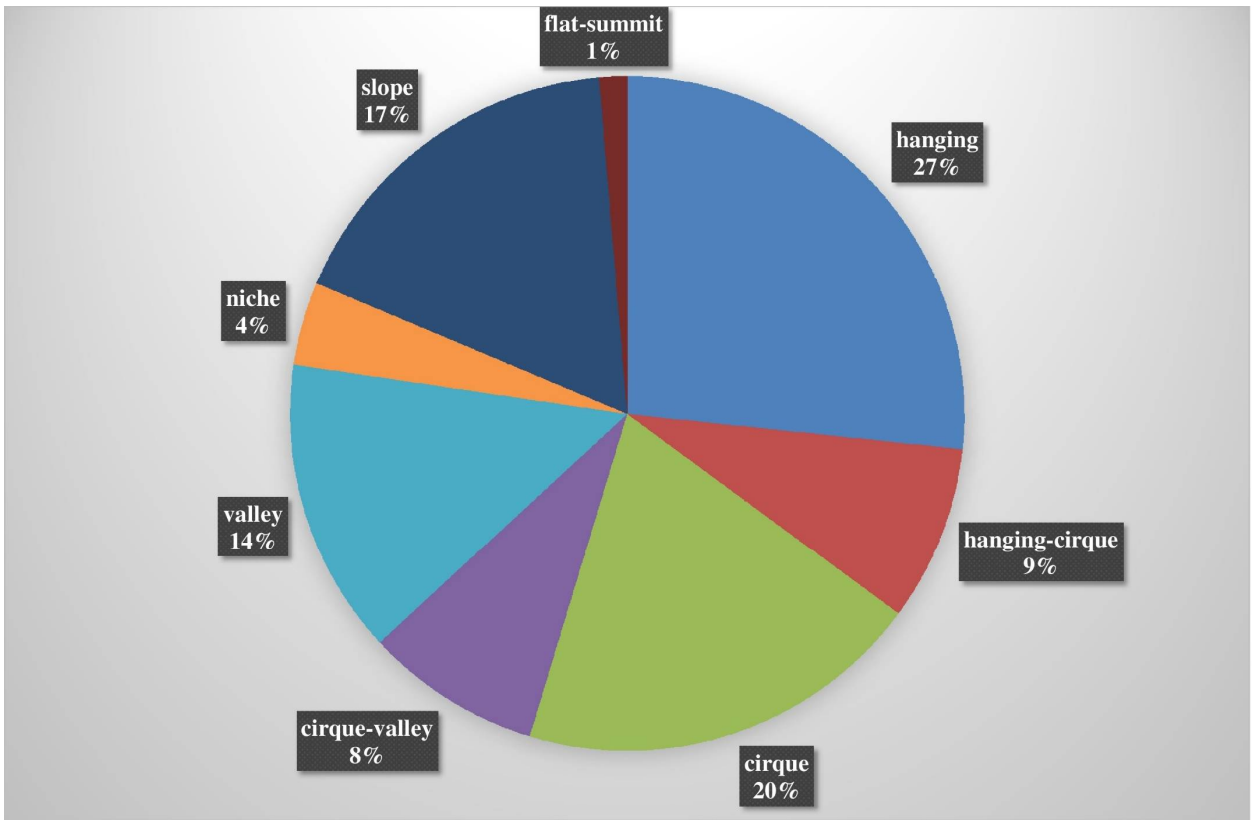

Fig. 5. Distribution of the number of glaciers in 2010 by morphological types

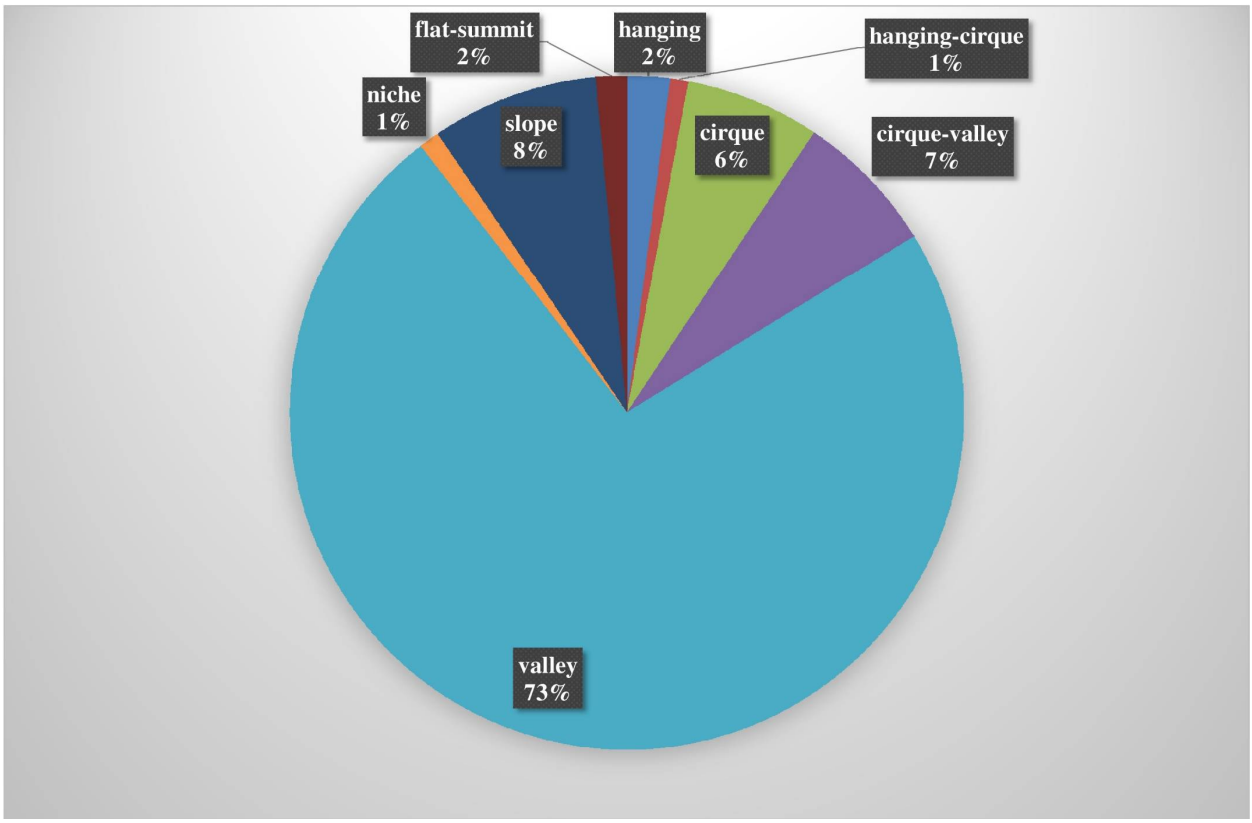

Fig. 6. Distribution of glacial areas in 2010 by morphological types

Preprints (www.preprints.org) | NOT PEER-REVIEWED | Posted: 18 August 2018 doi:10.20944/preprints201808.0332.v1

Peer-reviewed version available at Geosciences 2018, 8, 414; doi:10.3390/geosciences8110414

It should be noted that in different parts of the massif, the relationship between the morphological types of glaciers is also different. Valley glaciers are most developed in the highest, central part of the massif, slope glaciers predominate on the northern weakly dissected slopes, while small car glaciers dominate the lower eastern and southeastern periphery.

The aspect distribution of the number of glaciers (Fig.7) is quite typical for the study region: glaciers of the northeastern and northern slopes prevail. This position of the glaciers is most favorable both due to reduced insolation on shaded slopes, and thanks to the accumulation of snow that is swept to the leeward slopes by the prevailing south-western winds.

Nevertheless, the aspect distribution of glacial areas (Fig. 7) is more complex, with several peaks in the north-western, north-north-east, east-north-east (main) and southeastern (the least pronounced). Such a distribution, obviously, is determined by the complex geomorphological configuration of Tavan Bogd mountain massif with varying length and height of the slopes of different orientation.

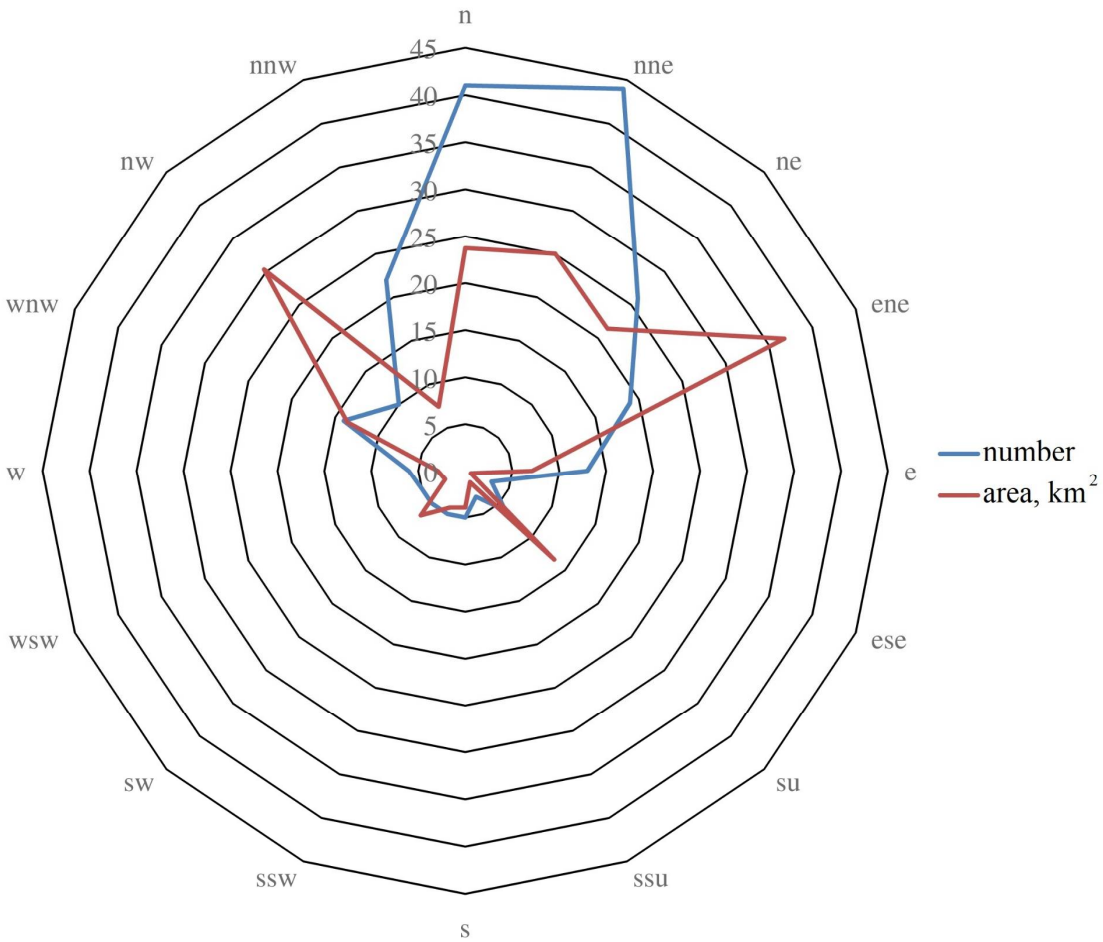

Fig. 7. The aspect distribution of the number and area of glaciers in 2010

Consideration of the specific features of glaciation of different river basins makes it possible to establish more precisely the aspect features of the glaciation of the Tavan-Bogdo massif (tab. 3). The total areas of the glaciers of the Tsagan-Gol (east-north-east exposure) and Sangadyr (west-north-western) expanses are approximately equal. Nevertheless, the average area of glaciers in the

Preprints (www.preprints.org) | NOT PEER-REVIEWED | Posted: 18 August 2018 doi:10.20944/preprints201808.0332.v1

Peer-reviewed version available at Geosciences 2018, 8, 414; doi:10.3390/geosciences8110414

basin of Tsagan-Gol is about 2 times larger, i.e. the glaciers themselves are larger here. On the contrary, ELA in the basin of the river. Sangadyr is about 150 m lower, which indicates a more abundant supply of glaciers. Obviously, the windward slopes of the massif receive significantly more precipitation than the leeward ones, and the transfer of snow to the leeward slopes is not enough to equalize differences in glacial accumulation. Geomorphological structure of glacial basins is the factor which equates the conditions for the existence of glaciers on the windward and leeward slopes. From the point of view of the extent of the mountain ridges, the basins of the Tsagan-Gol and Sangadyr rivers are in an equal position, as evidenced by approximately equal values of the glaciation intensity (average glaciation area per 1 km of the mountain ridge). But the area of the firn basin for Tsagan-Gol is much higher. To prove this fact, let us use the areas above the climatic snow boundary (the height from which, on horizontal areas, the accumulation on average exceeds the ablation for an average year). The best approximation to this theoretical indicator is the position of ELA on flat-topped glaciers, the surface slopes of which are minimal. Based on the ELA on the flat-topped glaciers of Tavan Bogd, this height can be drawn approximately at the level of 3500. As can be seen from Table 3, for the Tsagan-Gol basin, the area of territoty with a height of more than 3,500 m is almost twice as high as that for the Sangadyr River basin.

Tab. 3. Glacio-geomorphologic features of different river basins of Tavan-Bogd.

Basin	Aspect	Area, km^2	average area	Average weighted ELA	Intensity of glaciation	S3500, $км^2$
Kalguty	N	24,42	0,84	3346	0,51	9,17
Ak-Alaha	NNW	0,86	0,43	3071	0,15	0
Sangadyr	WNW	59,16	1,29	3208	1,09	18,5
Budiuhanasıhe	S	15,50	1,19	3165	0,50	2,92
Postigiyn-Gol	SE	26,53	0,62	3245	0,33	8,61
Arshan-Gol	ESE	0,88	0,18	3275	0,11	0
Mogotiyn-Gol	NE	1,61	0,23	3368	0,12	0
Ikh-Hatugiyn Gol	N	2,11	0,19	3335	0,09	0
Baga-Hatugiyn Gol	NNE	0,23	0,08	3348	0,09	0,55
Nalia-Gol	NNE	5,58	0,31	3293	0,37	0,55
Tsagan-Gol	ENE	61,41	2,36	3377	1,11	34,54
Ikh-Oygoryn-Gol	SE	1,78	0,10	3429	0,07	0,30
Shepk-Oygoryn-Gol	NNE	0,18	0,09	3267	0,08	0

S3500- area with altitudes over 3500 m a.s.l.

LIA reconstruction.

According to our reconstruction, in the maximum of the LIA, the glaciation of the Tavan Bogd massif was represented by 235 glaciers with a total area of 353.4 km. sq., which is about 1.8 times more than today. The estimated average glacier-weighted average ELA was 3235 m, which is about 50 m lower than at present. The lowest height of glacier spread was 2240 m (in the western

part of the massif), which is about 160 m lower than in 2010, the average height of the glacial snouts was 3025 m, which is about 110 m higher than in 2010.

The distribution of glaciers in size, despite the much larger average glacier sizes (1.45 km compared to 0.89 km in 2010) had a maximum LIA character similar to the modern one (fig. 8). The distribution of glaciers in size, despite the much larger average glacier sizes (1.45 km compared to 0.89 km in 2010) had a maximum LIA character similar to the modern one. Quantitatively, small glaciers predominated, although the maximum of their occurrence was shifted to a range of 0.1-0.5, i.e. A much smaller proportion of the glaciers on the verge of extinction. In terms of area, as in 2010, there were 2 maxima in the area intervals from 1 to 5 km and more than 10 km, although the dominance of the largest glaciers was more pronounced.

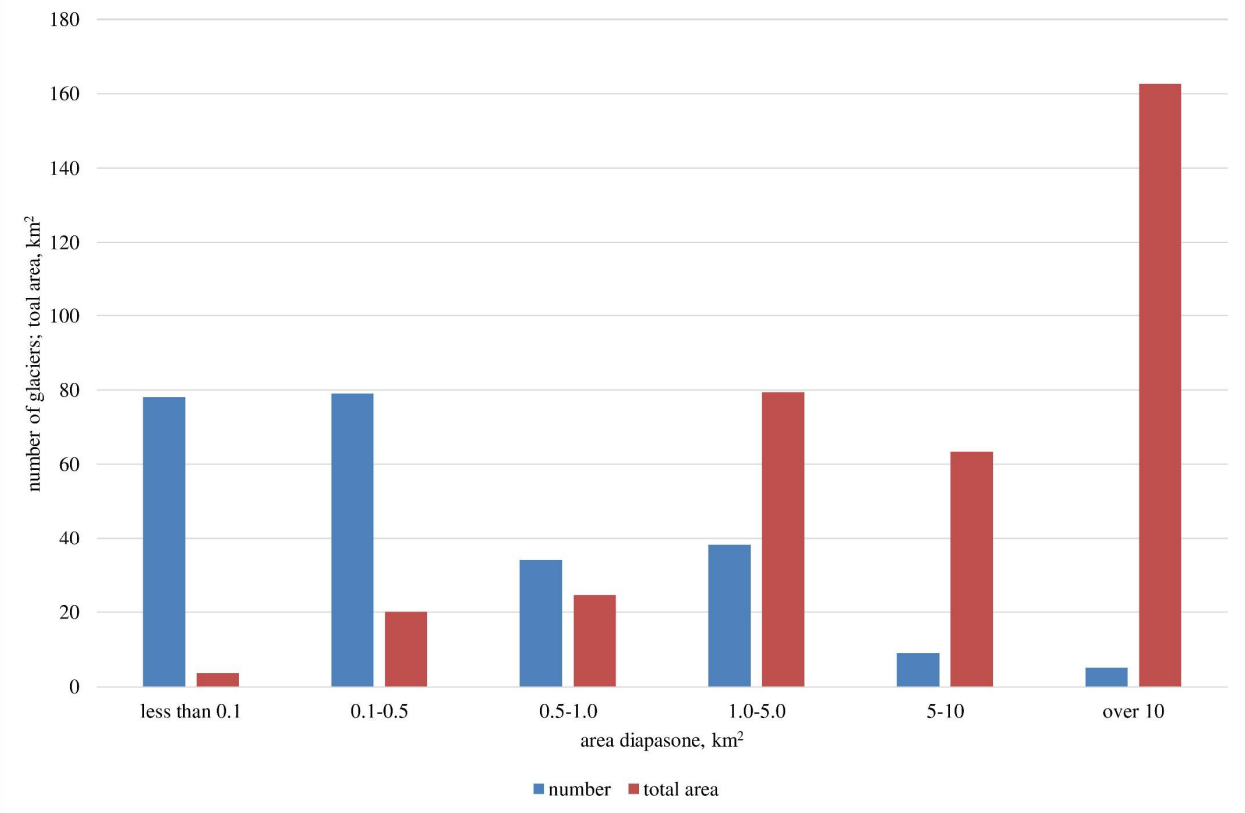

Fig. 8. Distribution of the quantity and total area of glaciers in the maximum of the LIA in different intervals of areas

The largest glacier of Tavan Bogd during this period was the Kanas glacier (66.85 km), considerably exceeding the area of the Potanin glacier (47.2 km), while the picture is now reversed (the Potanin-Alexandra glacier has an area of 36.84 km and the glacier Kanas 24.49 km). This fact nevertheless does not indicate the predominance of glaciers on the western slopes of the massif but is caused by the centripetal configuration of the valley of the river. Sangadyr, due to which the main glacial stream merged with glaciers of the tributary valleys.

The assumption that the glaciation of the western slopes of the massif in the LIA maximum was not dominant is confirmed by the aspect distribution of the number and areas of glaciers (Fig. 9). As at present, at this time the greatest number of glaciers was located on the northeastern and northern slopes, the maximum glaciation areas were situated on the northeastern, southeastern and western slopes.

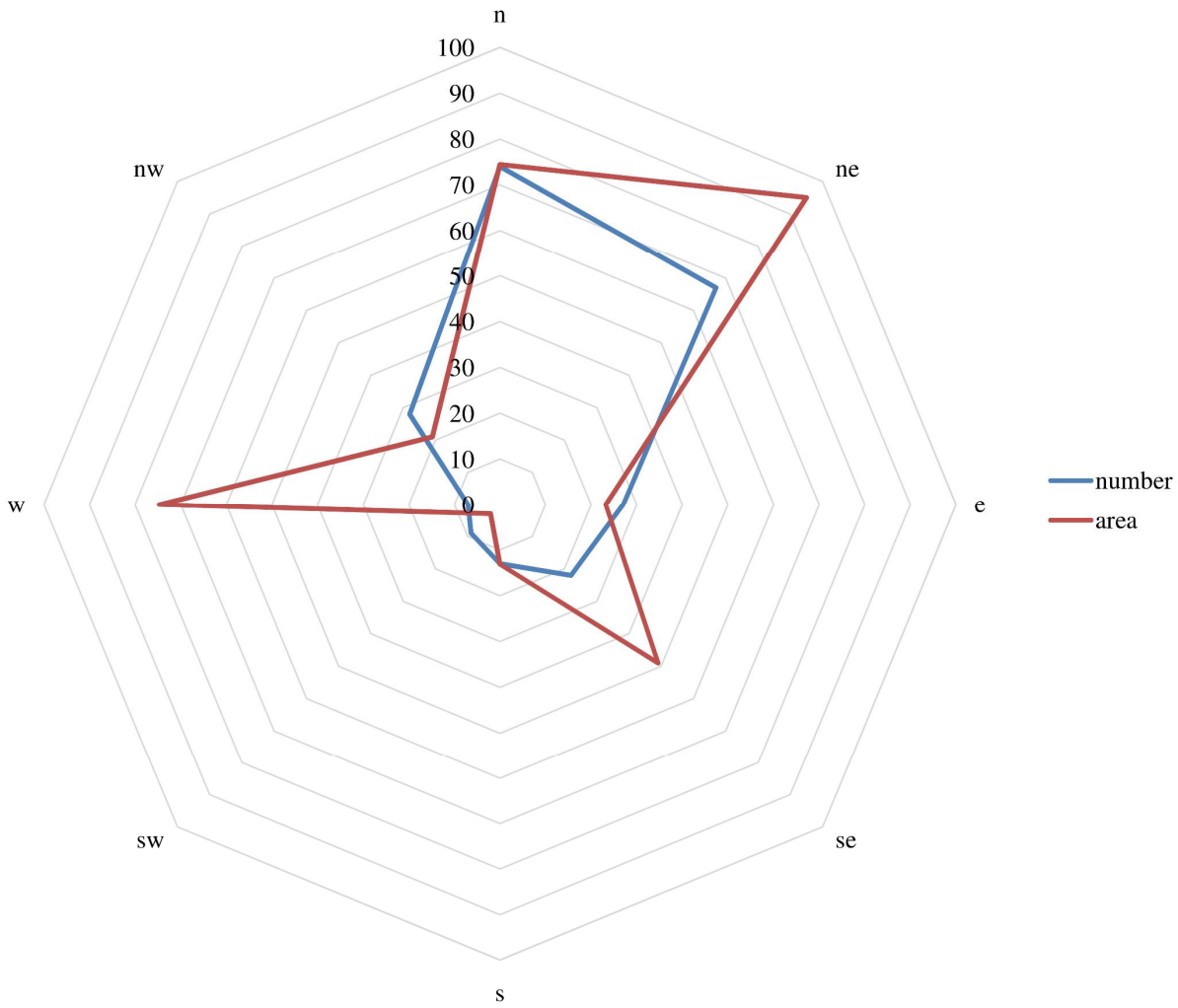

Fig. 9. The aspect distribution of the number and area of glaciers in the maximum of the LIA.

The morphological structure of the glaciation in the LIA maximum did not differ much from the current one. Valley and flat top glaciers had a somewhat larger proportion of the total quantity and total area of the glaciers, which reflects the greater development of large forms of glaciation (fig. 10, fig. 11).

Preprints (www.preprints.org) | NOT PEER-REVIEWED | Posted: 18 August 2018 doi:10.20944/preprints201808.0332.v1

Peer-reviewed version available at Geosciences 2018, 8, 414; doi:10.3390/geosciences8110414

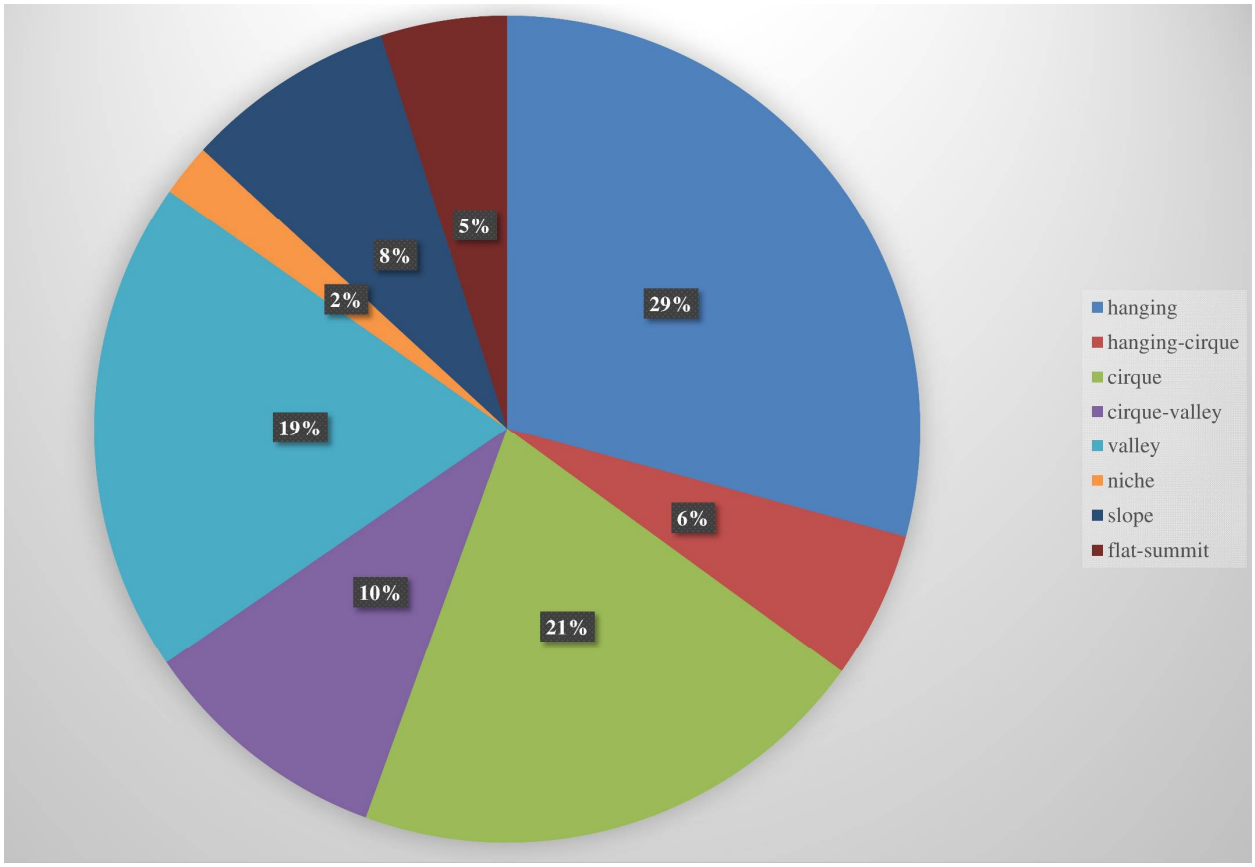

Fig. 10. Distribution of the number of glaciers in the maximum of the LIA by morphological types

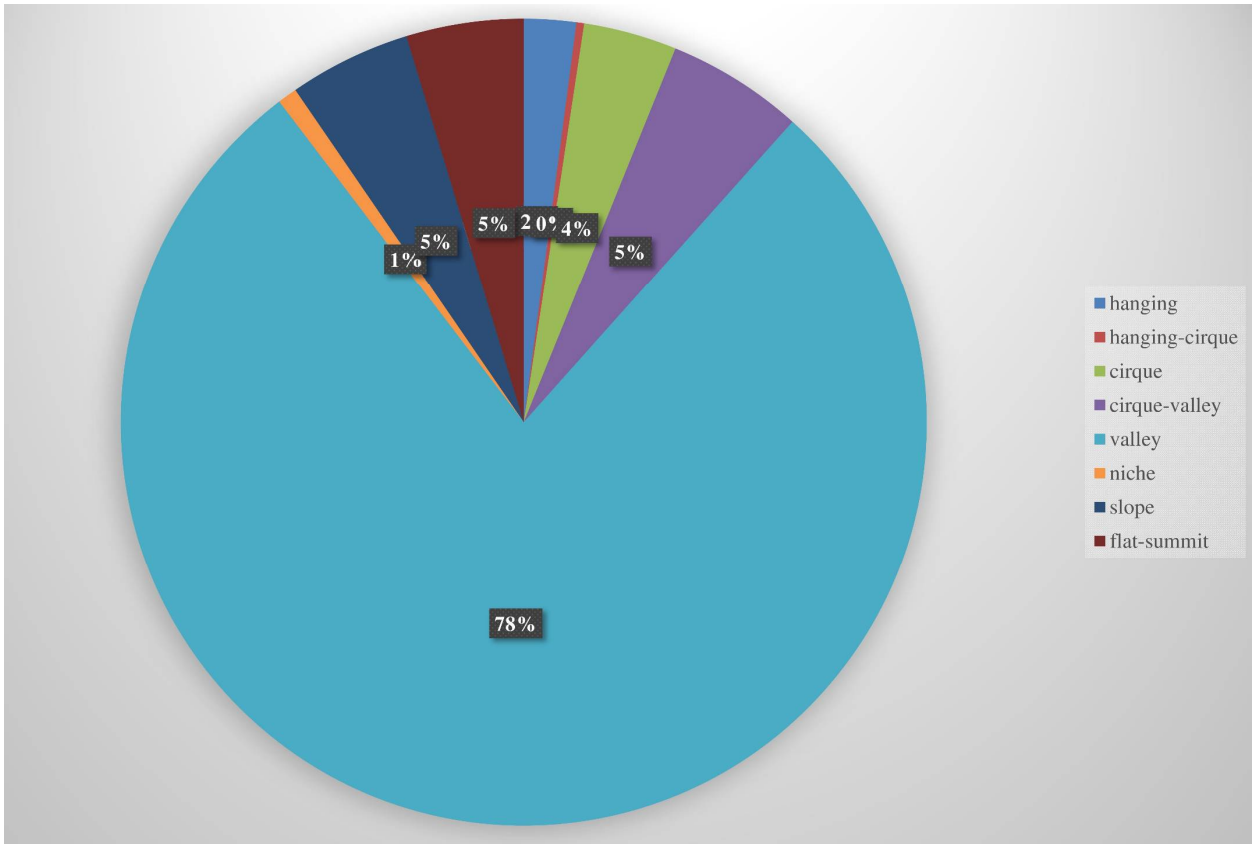

Fig. 11. Distribution of glacial areas in the LIA by morphological types

Preprints (www.preprints.org) | NOT PEER-REVIEWED | Posted: 18 August 2018 doi:10.20944/preprints201808.0332.v1

Peer-reviewed version available at Geosciences 2018, 8, 414; doi:10.3390/geosciences8110414

Glacial recession after the LIA maximum

After the LIA maximum the general tendency of glacial retreat resulted in 152.42[2] km loss of area by 2010, which makes about 43.1% of the total area (tab. 4). Glacial shrinkage was uneven: in 1820-1968 the total area of the glaciers decreased with rate of 0.74 km^2/year, in 1968-2010 the retreat speeded up to 1.02 km^2/year. This tendency is well seen in all the river basins of Tavan Bogd.

Tab. 4. Glacial shrinkage in different river basins after the LIA maximum.

	1820-1968		1968-2010		1820-2010	
Basin	Δ S, km^2/%	%/year	Δ S, km2/%	%/year	Δ S, km2/%	%/year
Kalguty	20.01/39.5	0.27	6.18/20.2	0.48	26.19/51.8	0.27
Ak-Alaha	2.16/61.0	0.41	0.52/37.7	0.90	2.68/75.7	0.40
Sangadyr	23.49/24.9	0.17	10.84/15.3	0.36	34.33/36.4	0.19
Budiuhanasıhe	9.20/31.4	0.21	4.65/23.1	0.55	13.85/47.2	0.25
Postigiyn-Gol	15.42/31.75	0.21	6.61/20.0	0.47	22.03/45.4	0.24
Arshan-Gol	0.79/34.8	0.24	0.60/40.5	0.97	1.39/61.2	0.32
Mogotiyn-Gol	2.15/37.4	0.25	1.99/55.3	1.32	4.14/72.0	0.38
Ikh-Hatugiyn Gol	5.12/60.31	0.41	1.26/37.4	0.89	6.38/75.2	0.40
Baga-Hatugiyn Gol	0.61/57.55	0.39	0.22/48.9	1.16	0.83/78.3	0.41
Nalia-Gol	4.87/41.3	0.28	1.35/19.5	0.46	6.22/52.7	0.28
Tsagan-Gol	20.78/23.1	0.16	7.72/11.2	0.27	28.50/31.7	0.17
Ikh-Oygoryn-Gol	4.18/59.9	0.40	1.02/36.4	0.87	5.20/74.5	0.39
Shepk-Oygoryn-Gol	0.60/69.8	0.47	0.08/30.8	0.73	0.68/79.1	0.42
Total or average	109.38/30.95	0.21	43.04/17.6	0.42	152.42/43.1	0.23

In the north-eastern periphery of Tavan Bogd large glaciers were absent even in the LIA maximum (fig. 12), glacial recession here was mostly expressed by the disappearance of small hanging and cirque glaciers (31 after the LIA maximum). If the rates of glacial retreat that took place in 1968-2010 remain in the nearest future, the glaciers here will disappear completely by 2060.

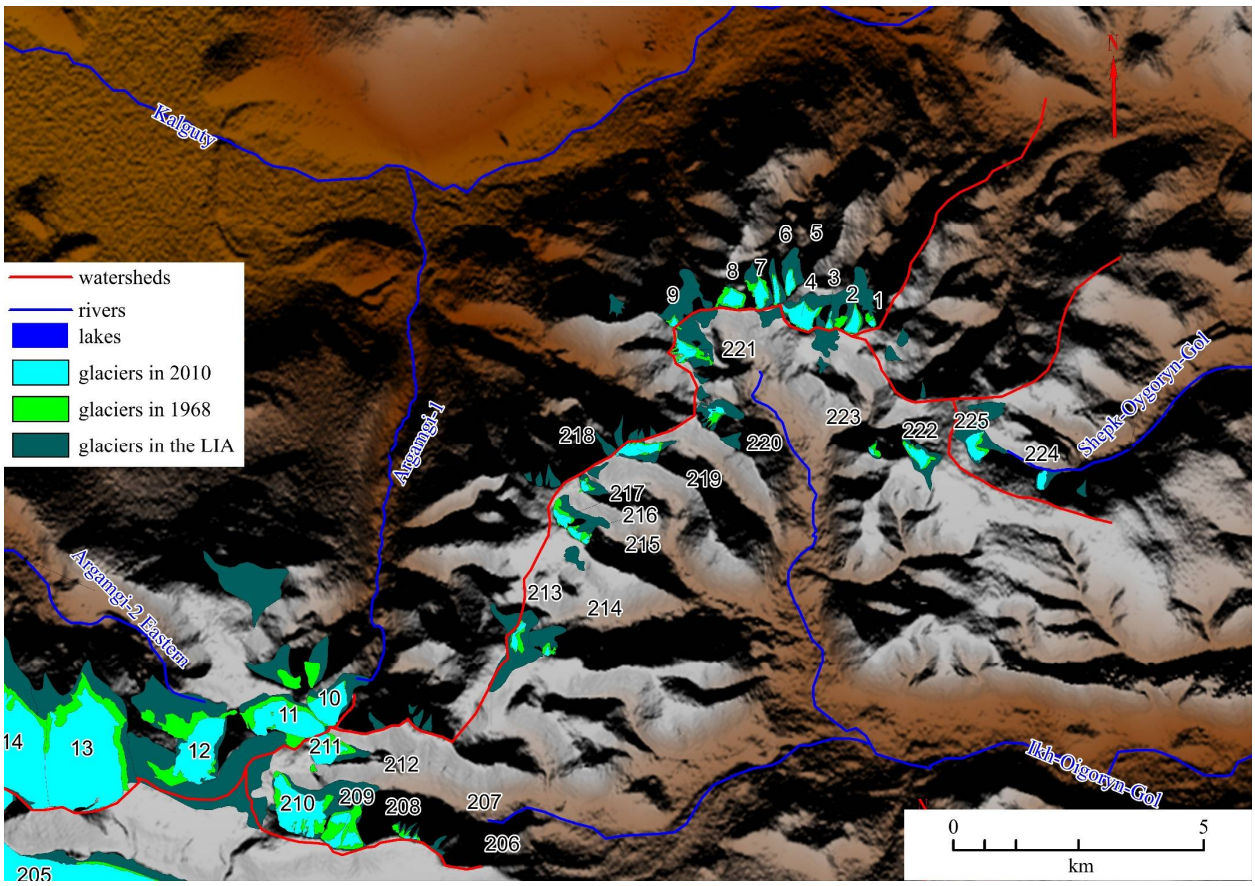

Fig. 12. Glacial shrinkage after the LIA maximum in the north-east of Tavan Bogd.

Similar situation took place in the north-western periphery (Kara-Chad and Ak-Alaha river basins, fig. 13). However, in the higher part of Tavan Bogd in the upper reaches of Agramgi-2 and Argamgi-3 the disappearance of the glaciers was not typical due to larger glaciers. Degradation of the glaciers here mostly happened in the form of retreat of the snouts of valley glaciers (No 20, 23) or complete disappearance of the snouts, resulting in disintegration of the valley glaciers or their transformation to other morphological types (No 12, No 14-16).

Preprints (www.preprints.org) | NOT PEER-REVIEWED | Posted: 18 August 2018 doi:10.20944/preprints201808.0332.v1

Peer-reviewed version available at Geosciences 2018, 8, 414; doi:10.3390/geosciences8110414

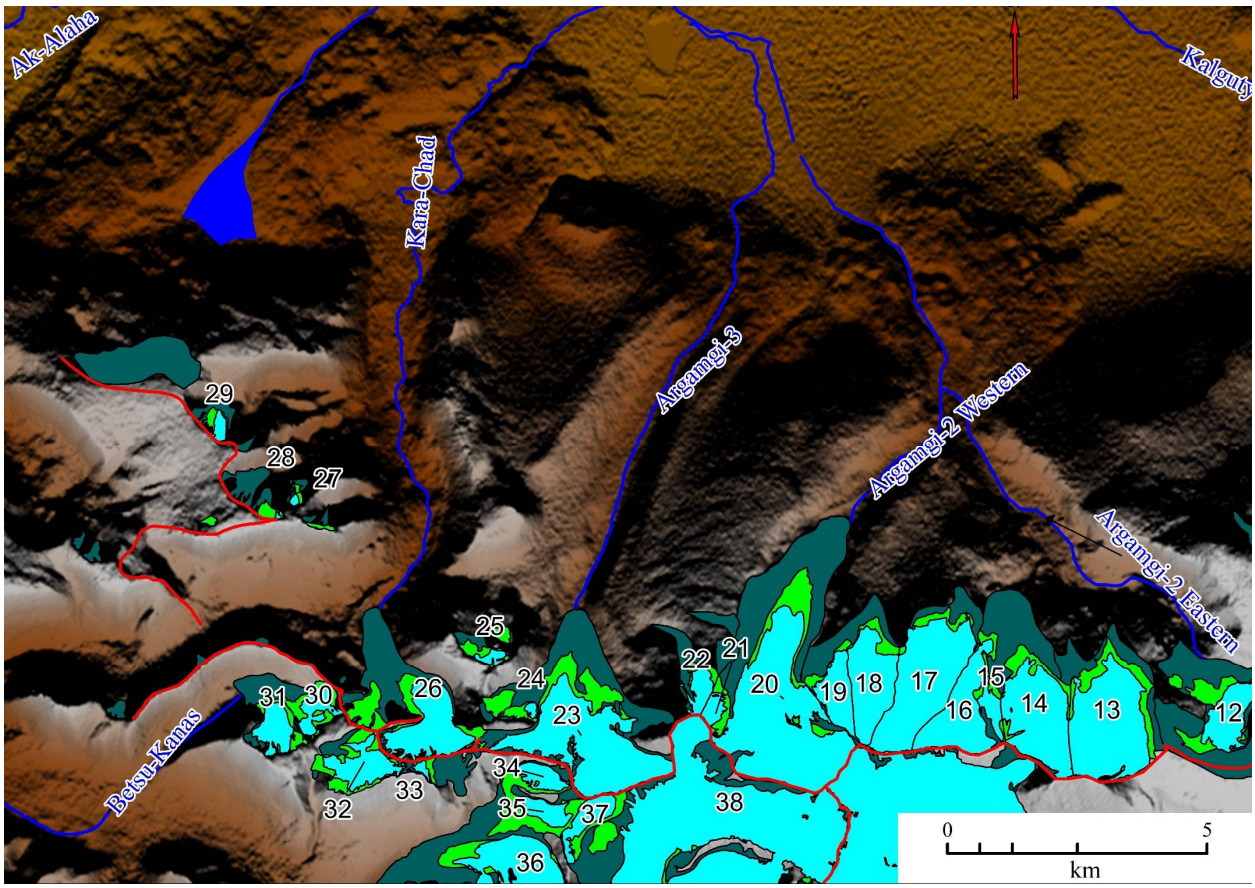

Fig. 13. Glacial shrinkage after the LIA maximum in the north-west of Tavan Bogd.

According to the information obtained for two largest glaciers of the northern slope of Tavan Bogd (tab. 5) they behaved synchronously. The periods of rapid retreat happened around 1968 and after 2009, slow retreat took place in the 1990-s. The recent fast degradation of the glaciers is supposed to be the delayed reaction to the period of rapid increase of the temperature in the 1990-s [67].

Tab. 5. Recession of the glaciers of the north slope Tavan Bogd.

Number (name) of the glacier	No 20 (Argamgi-2)	No 23 (Aramgi-3)
Time interval	Average rate of retreat m/year	
1820-1962	7.9[a]	4.5[a]
1962-1968	14.0[b]	35.0[b]
1968-1977	27.7[c]	8.9[c]
1977-1984	14.4[d]	12.0[d]
1984-1989	12,6[d]	4.0[d]
1989-2001	6.3[e]	5.4[e]
2001-2004	6.3[f]	14.5[f]
2004-2006	15.5[f]	5.0[f]
2006-2009	2.5[f]	15.3[f]
2009-2015	41.3[f]	22.3[f]
2015-2018	15.6[f]	21.6[f]

[a]- Paleoreconstructions and aerial images analysis, [b]- aerial and satellite images analysis, [c] satellite images analysis, [d]- satellite images and in situ observations of other authors [68] analysis, [e]- satellite images and in situ observations analysis, [f]- in situ observations

Preprints (www.preprints.org) | NOT PEER-REVIEWED | Posted: 18 August 2018 doi:10.20944/preprints201808.0332.v1

Peer-reviewed version available at Geosciences 2018, 8, 414; doi:10.3390/geosciences8110414

In the western part of Tavan-Bogd (fig. 14) disappearance of a group of small cirque glaciers on the watershed of Sangadyr and Budiuhansuhe rivers and the disintegration of a dendrite valley glacial system of Kanas were the main features of the glacial recession.

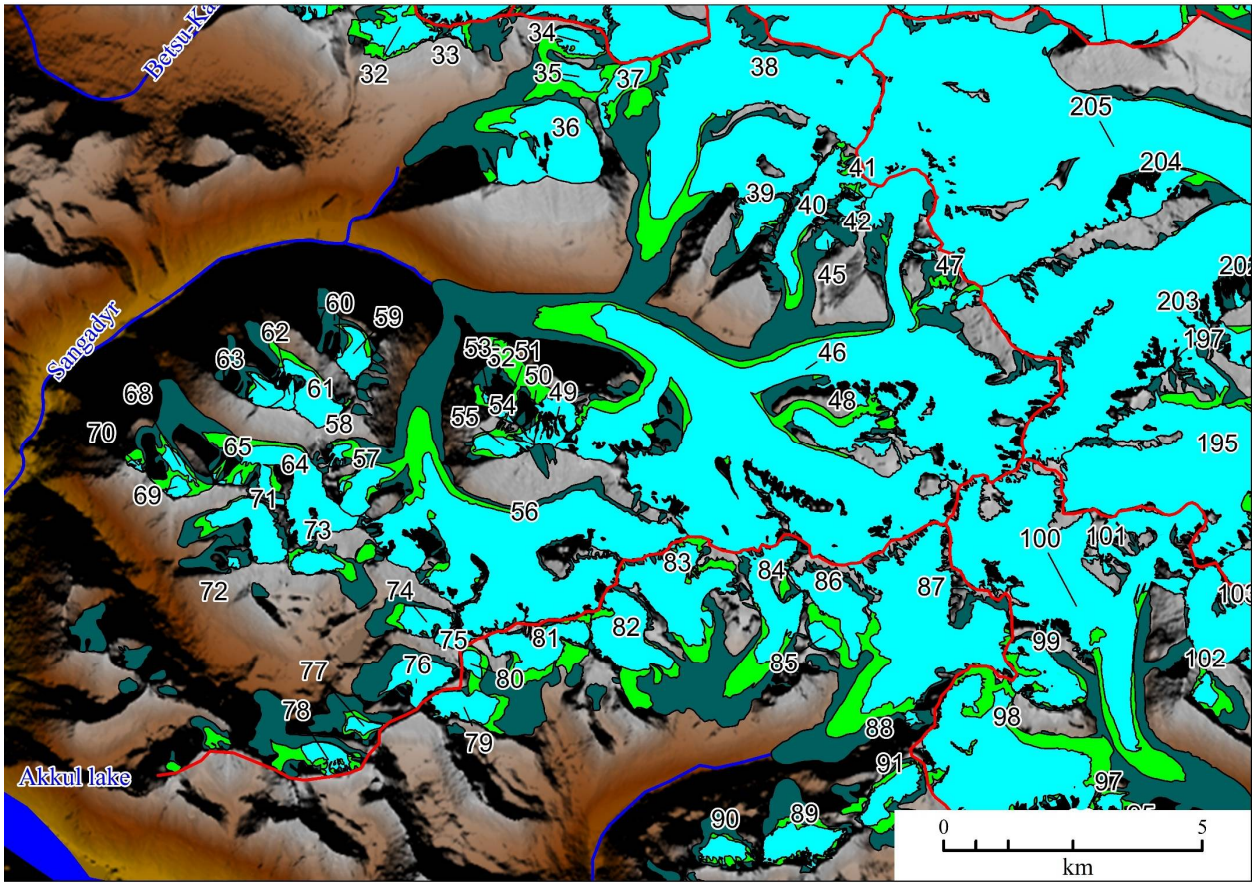

Fig. 14. Glacial shrinkage after the LIA maximum in the west of Tavan Bogd.

In the maximum of the LIA Kanas (Halasi, Przewalski) glacier was the largest (66.85 km^2) and the second longest (12.9 km^2) glacier of Tavan Bogd, its terminus reaching 2240 m a.s.l. By 2010 the main glacier lost 4 large tributaries, the total area of Kanas glacial system decreased to 47.5 km^2 (by 29%), the glacial terminus became 3.1 km shorter and its lowest point 250 m higher. The pattern of retreat of Kanas glacial terminus is similar to the one revealed for the glaciers of the northern slope: rapid retreat in 1968-1989, slower retreat in the 1990-s and an abrupt acceleration after 2006, speeding up to extremely high values in 2010-2018. Also, a longer range of observations gave the opportunity to reveal generally slow retreat in 1820-1909, fast retreat in 1909-1916, slowing down in 1959-1968. In recent years very fast glacial retreat is a sign of the further disintegration of the Kanas glacier and the loss of the next tributaries, primarily the lower south-western.

Tab. 6. Rates of retreat of Kanas (Halasi, Przewalski, No 46) glacier

Time interval	Retreat, m	Average rate of retreat m/year
1820-1909	434[g]	4.9
1909-1916	106[e]	15.1
1916-1959	1470[e]	34.2
1959-1968	90[d]	10.0

Preprints (www.preprints.org) | NOT PEER-REVIEWED | Posted: 18 August 2018 doi:10.20944/preprints201808.0332.v1

Peer-reviewed version available at Geosciences 2018, 8, 414; doi:10.3390/geosciences8110414

1968-1977	253[c]	28.1
1977-1980	81[d]	27.0
1980-1989	241[d]	26.7
1989-2000	200[c]	18.2
2000-2006	143[c]	23.8
2006-2010	164[c]	41.0
2010-2018	494[c]	62.3

a- Paleoreconstructions and aerial images analysis, b- aerial and satellite images analysis, c satellite images analysis, d- satellite images analysis and in situ observations of other authors [32], e- satellite images and in situ observations analysis, f- in situ observations, g- in situ observations of other authors [37] and paleoreconstructions, e- in situ observations of other authors [32,37,38]

On the eastern slope of Tavan Bogd (fig. 15), the complete disappearance of glaciers during the period under review was not a characteristic phenomenon, which is due to the predominance of large glaciers here. In addition, the prevalence of valleys parallel to each other, characteristic of the upper reaches of the Tsagan-Gol River, did not contribute to the detachment of tributaries from large glaciers, in contrast to the upper reaches of the Sangadyr river. The reduction of the Potanin-Alexandra glacier system, which is the largest on the eastern slope, corresponds to the regularities revealed by us for the glaciers of the northern and western slopes.

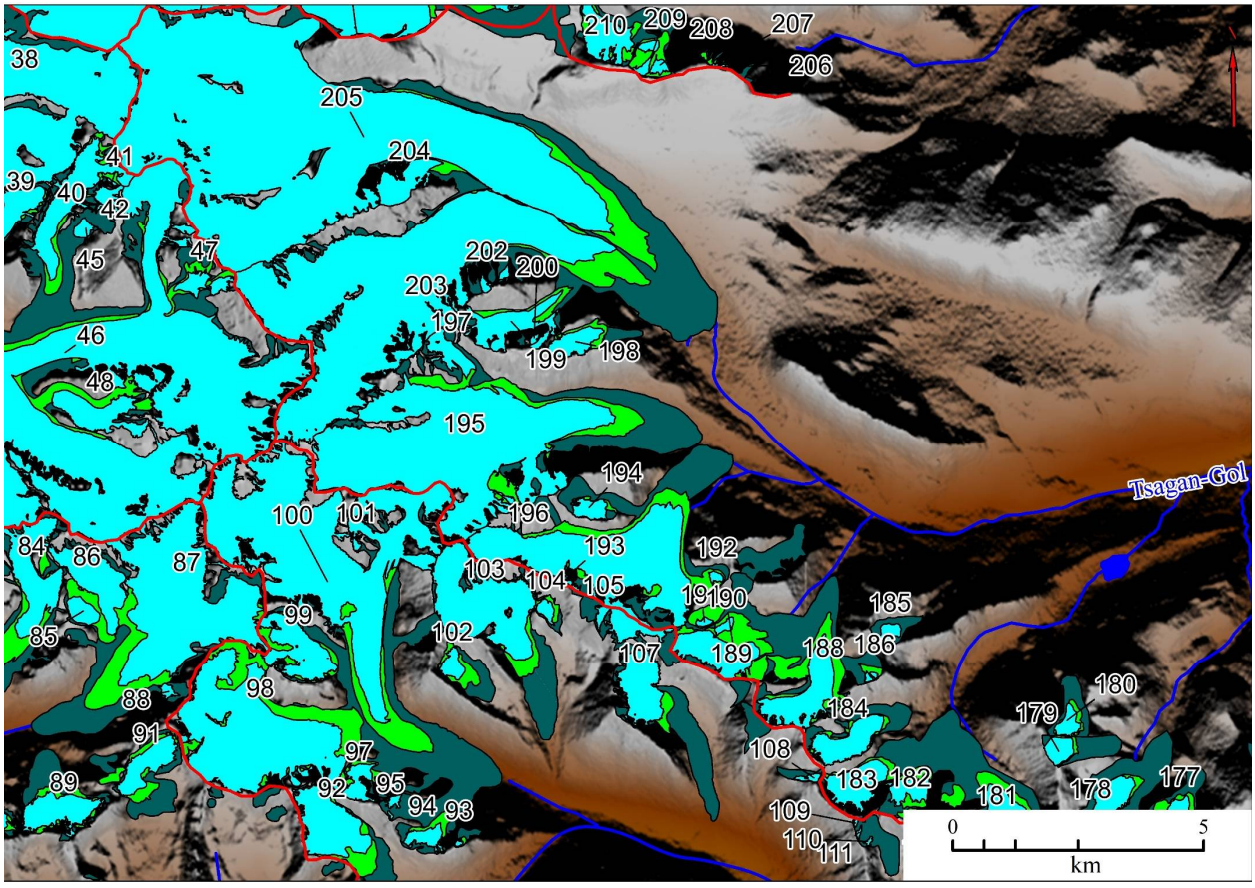

Fig. 15. Glacial shrinkage after the LIA maximum in the east of Tavan Bogd.

In the LIA maximum Potanin-Alexandra glacier reached the area of 47.42 km^2 it was the longest glacier of Tavan Bogd (about 13 km), its lowest point was at height about 2783 m a.s.l. By 2010 the glacier lost about 22% of its area, it became about 3 km shorter, its lowest point moved 110 m higher. This is similar to characteristics of retreat of Kanas glacier, though in fact Potanin and

Alexandra glaciers still have not completely separated from each other, forming a compound valley glacier. Though Potanin and Alexandra glaciers were not completely synchronous in their dynamics, generally several periods can be revealed: faster retreat around 1968, slower retreat in the 1990-s, followed by acceleration of retreat, reaching extremely high values in the last 8 years (tab. 7).

Tab. 7. Rates of retreat of Alexandra (No 203) and Potanin (No 205) glaciers.

Time interval	Total retreat of the glacier, m/average rate of retreat m year^{-1}	
	Alexandra glacier	**Potanin glacier**
~1820-1935	983/8.6[a]	1061/ 9.2[a]
~1935-1968	528/16.0[b]	422/12.8[b]
1968-1977	305/33.9[c]	271/30.1[c]
1977-1988	245/ 23.2[c]	299/27.2[c]
1988-1993	0/0[c]	206/41.2[c]
1993-2000	131/18.1[c]	112/16.0[c]
2000/2010	218/21.8[c]	185/18.5[c]
2010-2018	612/76.5[c]	498/62.3[c]

a- Paleoreconstructions and aerial images analysis [44], b- aerial and satellite images analysis, c satellite images analysis, d- satellite images analysis and in situ observations of other authors, e- satellite images and in situ observations analysis, f- in situ observations, g- in situ observations of other authors and paleoreconstructions, e- in situ observations of other authors

On the southeastern periphery of the massif (fig. 16) the glaciers from the LIA maximum have lost from 53 to 79% of the area. Disintegration of valley and cirque-valley glaciers led to present day dominance of small hanging and cirque glaciers in this part of Tavan Bogd.

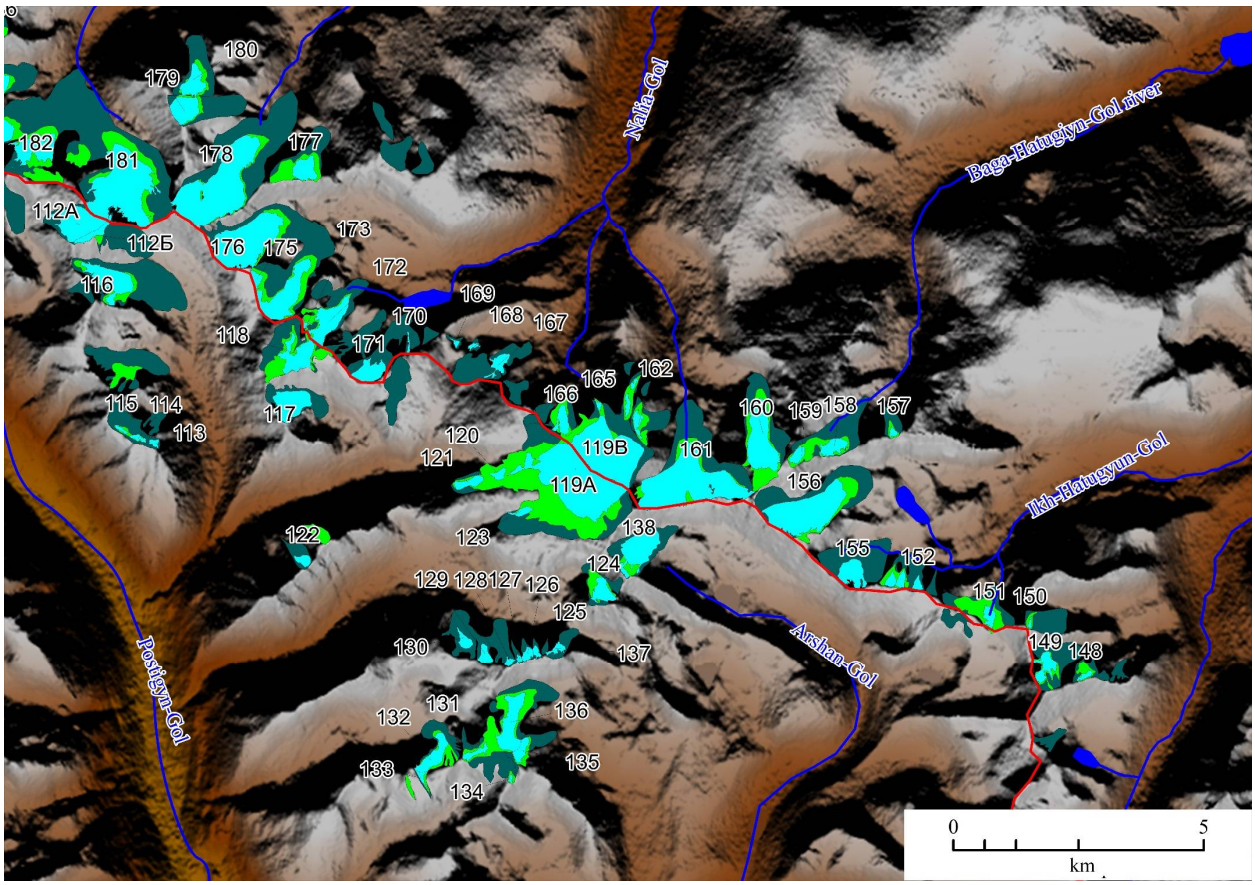

Fig. 16. Glacial shrinkage after the LIA maximum in the south-east of Tavan Bogd.

The most remote low-lying part of the southeastern periphery of the massif (the Mogotiyn-Gol river basin, Fig. 17) at the maximum of the LIA had a poorly developed glaciation of the cirque- and cirque-valley type. To date, only small cirque glaciers have been preserved here, the complete disappearance of which, while maintaining the same retreat rates, is a matter of one or two decades.

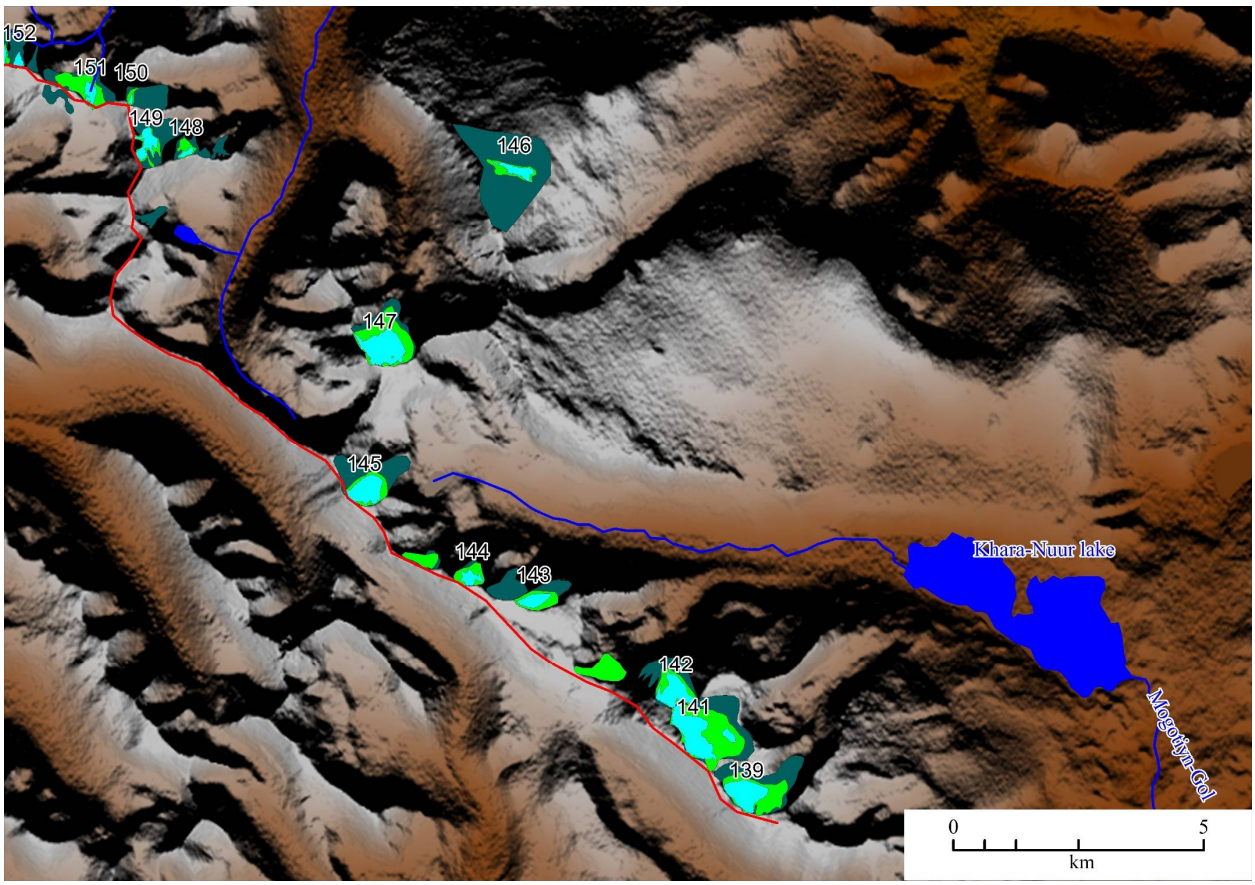

Fig. 17. Glacial shrinkage after the LIA maximum in the lowest part of the south-east of Tavan Bogd.

Summarizing the reconstruction of the dynamics of glaciers from the maximum of the LIA, we shall single out its main features.

1. There is a clear general tendency to glacial reduction, which is evident everywhere in Tavan Bogd, since 1968 the rate of glacial reduction has increased

2. The aspect of the slopes had little effect on the degree of glacier shrinkage. At the same time, there is a clear negative correlation between the size of the glaciers and the rate of degradation, due to which the glaciers of the relatively low periphery of Tavan Bogd have decreased to the greatest extent. This is clearly seen in the example of the relationship between the average area of glaciers in river basins in the Tavan Bogd area in the LIA and the reduction of their area in % (Fig. 18).

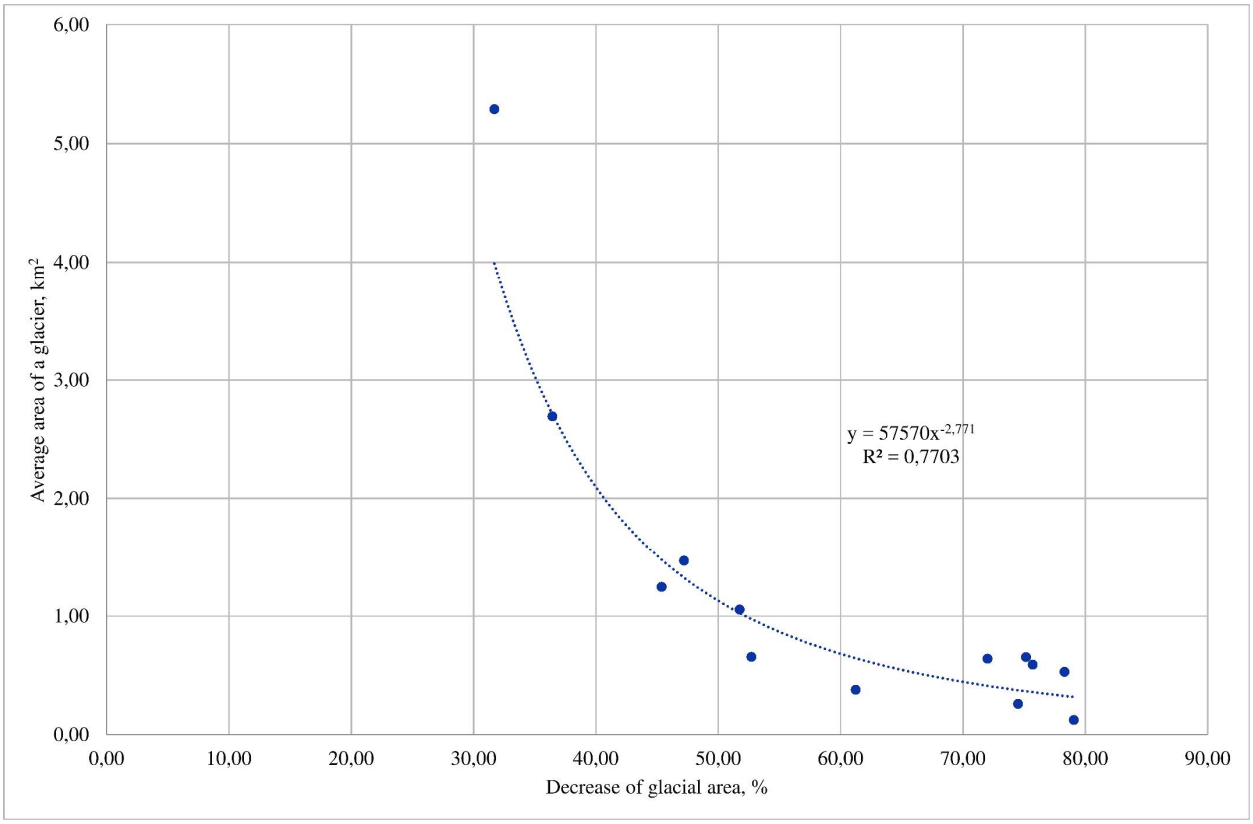

Fig. 18. Relationship between the average area of the glaciers in different river basins of Tavan Bogd in the LIA maximum and glacial reduction (%) from the LIA maximum and 2010.

3. Large valleys glaciers retreated unevenly, with a certain synchrony of their behavior noted. Fast retreat took place in 1968-1977 and after 2010, during the second period degradation of the glaciers was especially fast, reaching extreme values. In 1990-s the retreat was slow. To understand the reasons for this behavior of glaciers, it is necessary to consider the climatic data series for the relevant period. Unfortunately, in free access to data of meteorological stations are available only on the territory of China and the Russian Federation, obtaining information on the territory of Kazakhstan and Mongolia is difficult. In Fig. 19 data on the change in summer temperatures for three weather stations are presented. They characterize climatic conditions of the northern (Bertek), western (Altai, China) and eastern (Altai, Mongolia) slopes. Data on the Bertek weather station (closed in 1982) were extended based on data from the Kosh-Agach weather station, which were highly correlated with the Bertek data. The temperature changes are quite synchronous, although the general warming trend is less pronounced for the weather station Altai (China). Relatively warm conditions in the 1960s-1970s, a cold interval in 1981-1995, and very warm conditions after 1995 were distinguished. Proceeding from this, it is possible to assume the time of the reaction of glaciers to changes in summer temperatures in the range of 9-15 years. This assumption is proved by the mass balance calculations, that were done for the glaciers Argamgi-2 and Argamgi-3 [69].

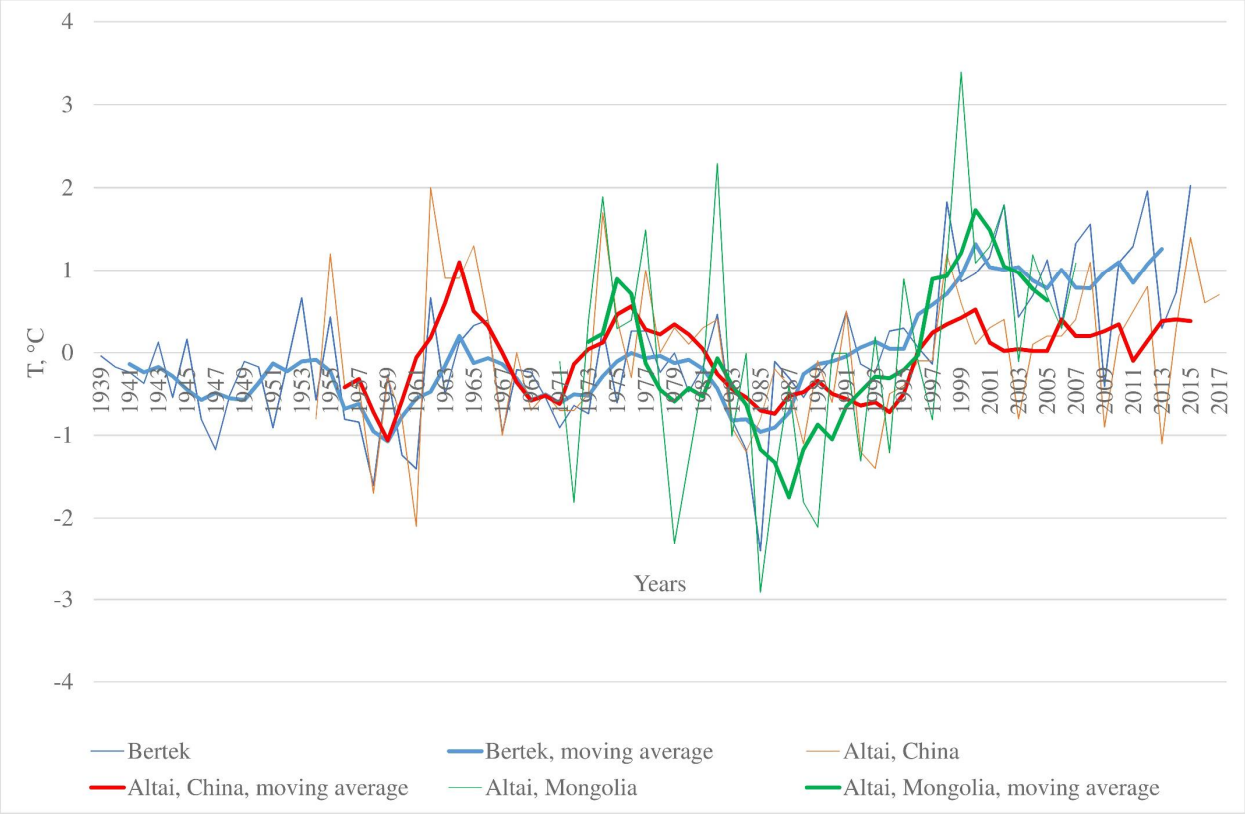

Fig. 19. Changes of average summer temperature (relative to multiyear average) for 3 meteorologic stations of Altai and 5-years moving average curves.

The second important climatic characteristic of the climatic conditions of the existence of glaciers is the annual amount of precipitation. The series of data on meteorological stations Katon-Karagai (northern slope), Altai (China) and Altai (Mongolia) were considered (Fig. 20). The change in the amount of precipitation on the northern and western slopes, according to meteorological stations, has an undeniable similarity: the presence of a trend of reduction of precipitation values until the mid-1970s and the subsequent gradual increase in precipitation. This correlates well with the acceleration of the retreat of glaciers in 1968-1977 and its slowdown in the 1990s. Afterwards, the sharp warming since the mid-1990s was more significant in its effect than a small increase in the amount of precipitation, which caused a rapid retreat of glaciers after 2010. Unfortunately, the data duration for the meteorological station Altai (Mongolia) is not long enough, in order to assess trends in precipitation change until the mid-1970s and there is no clearly defined trend in the subsequent period. But it is quite possible that the general trend of decrease of precipitation that was pronounced for the western and nortern slopes of the massive played the main role in the general trend of the glacial retreat in that period, because there was no warming trend until the 1990-s.

Preprints (www.preprints.org) | NOT PEER-REVIEWED | Posted: 18 August 2018 doi:10.20944/preprints201808.0332.v1

Peer-reviewed version available at Geosciences 2018, 8, 414; doi:10.3390/geosciences8110414

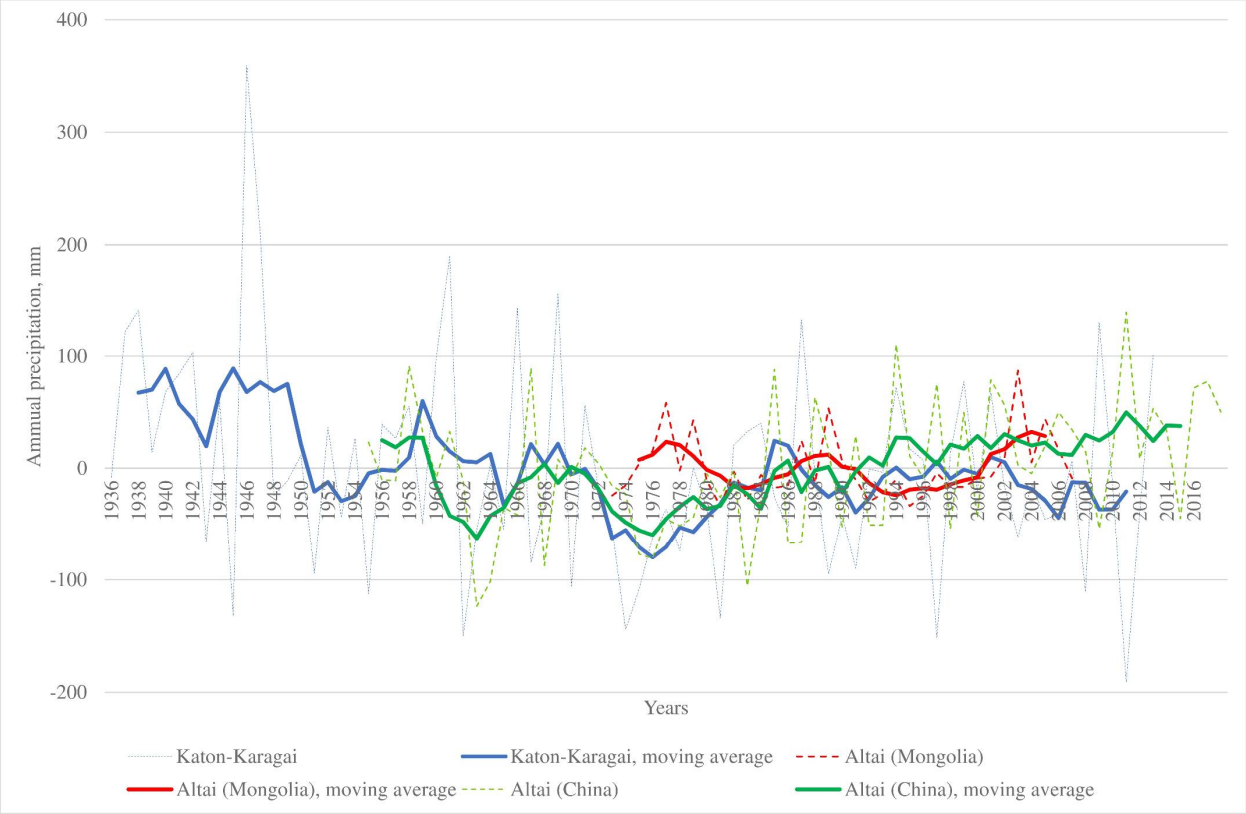

Fig. 20. Changes of annual precipitation (relative to multiyear average) for 3 meteorologic stations of Altai and 5-years moving average curves.

4. Discussion.

4.1. Recent glaciation of Tavan Bogd and comparison between different estimations and inventories.

According to our results in 2010 the glaciation of Tavan Bogd was represented by 225 glaciers with total area 200.98 km^2. The average weighted ELA is 3285 m a.s.l. The area of glaciers in the territory of Russian Federation is 25.28 km^2, 75.39 km^2 of glacial area is situated in the Chinese territory, 100.31 km^2 in the Mongolian part of Tavan Bogd. This study presents the first detailed analysis of the current structure of the glaciation of the entire Tavan Bogd massif.

Table. 8. Estimation of area of glaciation of Tavan Bogd by different authors.

Studied part of Tavan Bogd	source	Total area, km^2	Year	Source
complete	[44]	222.3	1987	Satellite and aerial imagery, route observations
Mongolian Part	[43]	94	?	Aerial imagery
Mongolian Part	[70]	134	1967-1978	Topographic maps 1:200000
complete	[71]	204	2009	Satellite imagery
Mongolian Part	[50]	79.77	2000	Satellite imagery
Mongolian Part	[34,72]	99	2013	Satellite imagery

Peer-reviewed version available at Geosciences 2018, 8, 414; doi:10.3390/geosciences8110414

In addition, data on the investigated glaciers were obtained for the northern slope within the framework of the RGI 5.0 / GLIMS database [73,74] for the northern slope of Tavan Bogd and the 2nd Glacier Inventory of China [75] for the western slope, although no special survey or an article devoted to these results for Tavan Bogd has yet appeared..

Differences in the estimates of areas of glaciation obtained by us and other researchers are due to several reasons.

1. Difference of source materials. Various authors used topographic maps, aerial photographs, space images, in some cases these materials were used in combination with the results of route observations. The least reliable sources are topographic maps, usually not detailed enough to accurately determine the boundaries of glaciers. In addition, maps of this territory were compiled as of 1960-1970, using aerial photographs. Aerial photographs, in turn, give significant distortions in the shape of glaciers, which sometimes leads to significant errors. Many of the estimates of modern glaciation are obtained from old materials that do not correspond to the present state ща the glaciers.

2. Different methodic used. For example, the authors [34] mapped only the open parts of the glaciers, without the moraine cover. Also, different lower limits of the glacier isolation area were used, from 0.01 to 0.1 km.

3. Uncertainty in the definition of the lower boundary of the glacier, especially in areas of glacier coverage by moraine material. This problem is exacerbated when working with Landsat 2.4, 5 images, which have relatively low resolution. The problem is solvable if further interpretation of other images with close acquisition dates is made, as well as in the coming years before and after the acquisition date. When considering the maximum number of images and creating long time series, the errors of individual years are compensated and reduced to a minimum. In addition, ground-based observations are a good way to correct the results. In the case of our work, the position of the boundaries of the glaciers of the northern slope of Tavan Bogd in the past 19 years has been adjusted in this way.

4. The difference between perennial snowfields and small glaciers is not always clearly seen in satellite images, and the same objects can be treated differently by one or the other class of objects. Such diagnostic signs of glaciers as crevasses and presence of zones of accumulation and ablation.

5. Differences in the delineation of ice divides in the areas of development of continuous ice cover at the borders of different river basins. In solving this problem, the use of Digital Elevation Models, which significantly more accurately display the relief in comparison with topographic maps, helps significantly.

In our previous article [67] we gave an example of differences between our results of delineation of the glaciers of the northern slope of Tavan Bogd and the results from the RGI 5.0 / GLIMS database [73,74].

In this article we will consider, as an example, the contours of glaciers according to the Second Catalog of China Glaciers (for 2006) and according to our data (fig. 21). In general, the contours of the glaciers are in good agreement with each other. Nevertheless, in the 2nd Glacier Inventory

of China the glacial outlines are more generalized, and the shape of glaciers is simplified. This is especially true of the food zone. For example, in the contours of the glaciers of the second Chinese catalog, many nunataks are not shown (Kanas Glacier, No 46). This is probably due to the fact that the creation of the 2nd Glacier Inventory of China used Landsat 2006 images for this territory, with a lower resolution than the Spot 5 images that we used. probably, for this reason, on some sites, the differences in the allocation of glaciers turned out to be drastic. For example, there are no small glaciers 41-44 (total area 0.22 km) marked by us in the north of the site in question in the Chinese catalog. In contrast, the glacier in the Chinese catalog to the west of the Glacier Kanas, having an area of 1.78 km, correspond to small glaciers 49-55 with a total area of 0.67 km in our catalog. As can be seen from the fragment of the Spot 5 satellite image, by 2010 there was no single glacier, in place of its snout there was a moraine complex or a rock glacier. To verify, we used a Landsat 7 image 2000-08-07 with a resolution of 15 m and made sure that the language of a single glacier was not available by the year 2000.

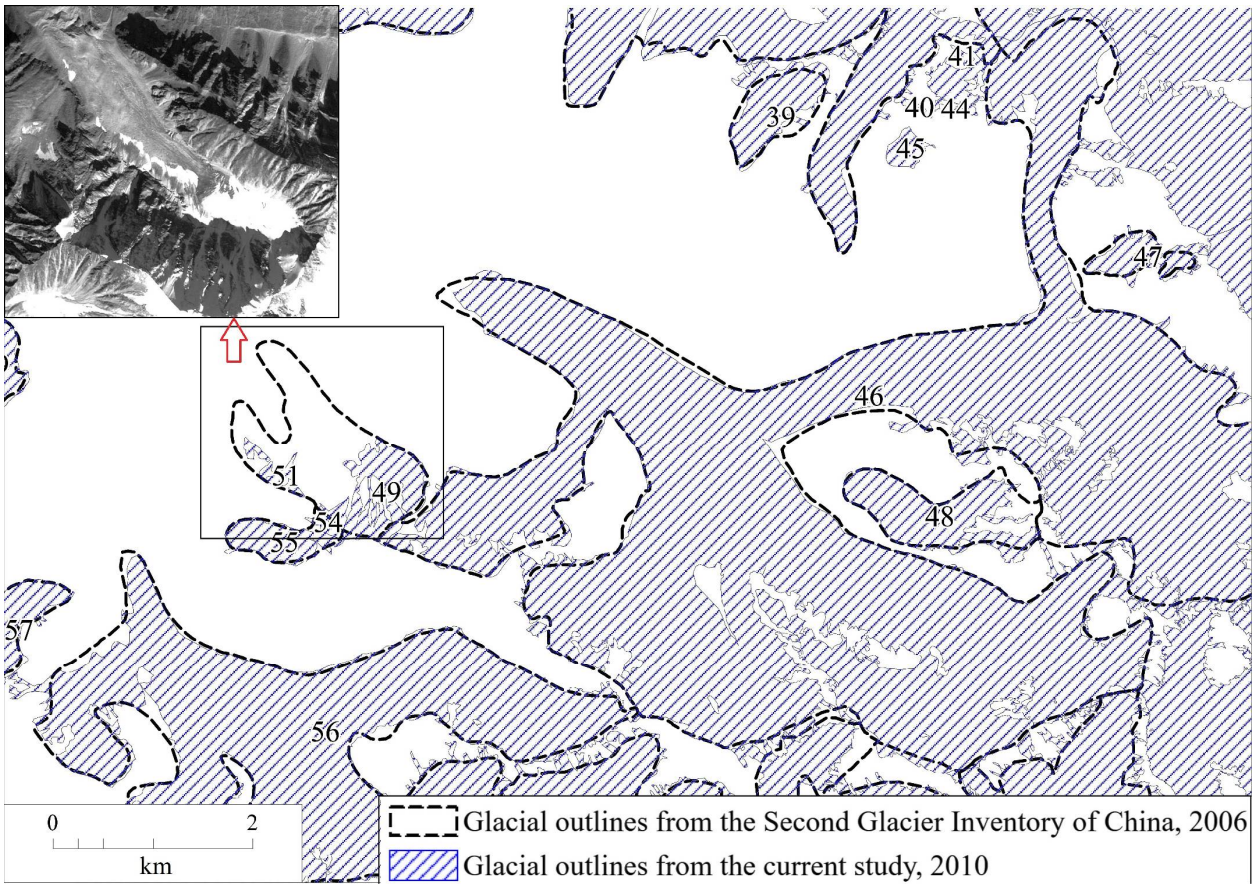

Fig. 21. Comparison of the contours of glaciers in the basin of the Sangadyr river, obtained by us with the contours from the Second Glacier Inventory of China (This data set is provided by Cold and Arid Regions Science Data Center at Lanzhou (http://westdc.westgis.ac.cn)). In the upper left corner- a fragment of SPOT 5 satellite image (2010).

4.1. Glacial recession after the LIA

According to our reconstruction, in the period from the maximum of the LIA, there was a 43% reduction of the area of glaciation of the Tavan Bogd. About 31% area loss took place by 1968, 12% - in the period 1968-2010 (about 2 times faster than in the period from the LIA maximum to 1968). The estimated area-weighted average ELA uplift was about 50 m

Comparison with the other mountainous area of the World shows similarity of processes and their scale. There is a tendency of increase of glacial recession beginning from the last quarter of the XX century. For example, the European Alps have experienced a 50% decrease in ice coverage in 1850-2000, the area loss over each decade (in percent) between the 1970s and 2000 was almost three times greater than the related loss of ice between 1850 and the 1970s [76]. In northern Norway there was a steady reduction in area (~0.3% a−1) between the LIA maximum (~1915) and 1988, recession paused between 1988 and 2001, the rate of recession accelerated to ~1% a−1 between 2001 and 2014 [21].

In the arid mountainous areas glaciers demonstrate roughly the same character of dynamics. The glacier retreat in the tropical Andes over the last three decades is unprecedented since the maximum extension of the LIA (mid-17th–early 18th century). In terms of changes in mass balance, the trend has been quite negative over the past 50yr, with a mean mass balance deficit for glaciers in the tropical Andes that is slightly more negative than the one computed on a global scale. A break point in the trend appeared in the late 1970s with mean annual mass balance per year decreasing from −0.2mw.e. in the period 1964– 1975 to −0.76mw.e. in the period 1976–2010. The retreat was much more pronounced on small glaciers at low altitudes [23]. Evaluation of the recession of Akshiirak and Ala Archa glacial centers, Tien Shan, central Asia, showed that the area shrinkage of Akshiirak and Ala Archa was 4.2% and 5.1%, respectively, from 1943 to 1977, and 8.7% and 10.6%, respectively, from 1977 to 2003. [24]. In the eastern Terskey–Alatoo Range, the Tien Shan Mountains, mapping of 109 glaciers using the 1965 1:25,000 maps revealed that glacier surface area decreased by 12.6% of the 1965 value between 1965 and 2003 [77].

In the area of research in most cases the reconstructed values of glacial shrinkage after the LIA demonstrate higher values. For example Lehmkuhl [14] on the basis of field work 1995-1998, topographic maps on a scale of 1:100,000 from 1948 and aerial photographs from 1991 estimated glacial area decrease of Turgen mountains by 56% and 56% Kharkhiraa mountains, snowline elevation was estimated about 80m.

Some of the results of the previous studies of the LIA glaciation shrinkage included parts of Tavan Bogd. Recently we obtained information about the glacial recession after the LIA maximum from the different glacial centers of the SE Altai, including the north slope of Tavan Bogd and half of its Mongolian part (Nairamdal ridge) (tab. 9) [78]. Comparison shows that the glacial decrease for Tavan Bogd was generally lower than for the other glacial centers of the region. Possible reasons for this phenomenon are the larger dimensions of the Tavan Bogd glaciers combined with large absolute heights of thire orographic base.

Table 9. Reconstructed LIA glazierisation of different glacial centres and its changes till present (2002-2013)[78].

Glaciation center	S, km^2	N	A (%)	ΔS, %	Δ ELA, m
Mongun-Taiga	49.5	87	NE (30)	59	120
Tsagan-Shibetu (south slope)	3.14	17	SE (34)	98	120
Turgen	62.1	94	N (34)	48	35

Preprints (www.preprints.org) | NOT PEER-REVIEWED | Posted: 18 August 2018 doi:10.20944/preprints201808.0332.v1

Peer-reviewed version available at Geosciences 2018, 8, 414; doi:10.3390/geosciences8110414

Glaciation center	S, km^2	N	A (%)	ΔS, %	Δ ELA, m
Kharkhiraa	78.8	85	NE (53)	58	60
Talduayr	3.1	4	N (63)	63	130
Mongun-Taiga Minor	2.1	6	NE (90)	60	15
Chihacheva ridge (Ikh Turgen)	59.1	93	NE (34)	51	65
North-western Saylugem (Jumaly and Usay river basins)	1.54	14	NE (95)	100	110
Saylugem	15.85	50	N (32)	76	80
Tavan Bogd (north slope)	39.8	9	N (79)	40	50
Nairamdal (north slope)	126.3	46	NE (35)	43	130
Sogostyn-Nuru	2.02	22	N (31)	88	80
Tsengel Khairkhan	33.18	69	NE (47)	69	70
Hunguyn-Nuru	20.51	41	N (60)	59	76
Sair	13.34	23	NE (55)	50	65
Tsambagarav	128.4	73	N (32)	44	90

Remarks. ΔS (%)- changes of glacial area from the LIA. Other symbols see in tab. 2.

According to the data from the comparison of aerial photographs with field data, the reduction of the glaciers of the northern slope of Tavan Bogd was estimated 24.3% [48], the data from this study has been used in the current article (valley glaciers of the north slope retreat estimations).

Chinese researchers basing on statistical analyses of the field data revealed a linear relationship exists between LIA area and that of modern glaciers from the time of the LIA to the middle of the 20th century (1950s through the 1980s) found out that glaciers in western China lost a total area of about 26.9%, but in the Ob river basin this shrinkage was higher (47.5%) [79]. Unfortunately, no statistics about the glacial shrinkage in the Ob basin after the middle of the 20th century is given.

Wang et. al found that glaciers in the Altai Mountains were in a state of retreat from 1959 to 2000 based on topographic maps and Landsat ETM images. The annual shrinkage rate was 29.94% by area, and the total area of the Kanas Glacier decreased by 4.21% with an annual rate of 0.0011 km^2 a−1. [80]. Another group of scientists using topographic maps in 1959 and ASTER remote sensing data in 2008 for the Friendship Peak in the Chinese Altai Mountains found out that the collective area of 201 glaciers between 1959 and 2008 was reduced by 30.4%. Fifty-five glaciers disappeared entirely. The average rates of reduction in area of glaciers with sizes less than 0.5, 0.5–1, 1–4, 4–10, and over 10 km^2 were 25.9%, 30.8%, 30.9%, 35.9%, and 27.4%, respectively [81]. This is different from our results for 1968-2010 (38% for the whole Tavan Bogd and 47% for the Chinese part of Tavan Bogd), which is not surprising taking into account that the glaciers studied by Wang et. al included also glaciers of South Altai Ridge and Mongolian Altai.

4.2. Retreat of glacial fronts.

Information on the change in the position of the ends of glaciers is of particular value, since it often contains information on periods beyond the time frame of aerial and space imagery. On the other hand, it is difficult to create a continuous and continuous series of data because of the remoteness of the study area and the difficulties of its field study, the large intervals between visits to glaciers, the lack of information on the position of the benchmarks, their possible destruction or displacement by exogenous processes. It seems promising to link these series to the earliest aerial photographs and space images, allowing both to extend and detail them, and to eliminate errors.

Solomina [82] analyzed materials on the retreat of about 1000 glaciers located in the mountain ranges of the former Soviet Union (Caucasus, Polar Urals, Pamir-Alay, Tien Shan, Altay, Kodar, Cherskiy range, Suntar-Khayata, Koryakskoye Nagorye, Kamchatka) between the LIA maximum and the second half of the XX century and found out that the scale of glacier shrinkage is much smaller in continental Siberia than in central Asia and along the Pacific margins. For Altai the magnitude was from 90 m to 2300 m, with median 458 and mean 558 m. For the 5 glaciers that we studied the retreat of the terminus between the LIA and 2000-2001 was from 1207 m to 2875 average 2068 m, being closer to the values for Central Asia. Probably, this is because Tavan Bogd is situated on the order of Siberia and Central Asia.

In the eastern Terskey–Alatoo Range, the Tien Shan Mountains,Detailed mapping of 10 glaciers using historical maps and aerial photographs from the 1943–1977 period, has enabled glacier extent variations over the 20th century to be identified with a higher temporal resolution. Glacial retreat was slow in the early 20th century but increased considerably between 1943 and 1956 and then again after 1977. The post-1990 period has been marked by the most rapid glacier retreat since the end of the LIA [77] .

In Altai most information is available for its Russian part. In the Katun'-Chuya glacial center after the last advance of the LIA, there was a general retreat with periods of oscillations in 1911–1914 and 1927–1930 [83]. Nikitin and Narozhnyj noted that oscillations took place in 1979–1980, 1987–1988, and 1993 [84]. On the background of a general retreat, the Right Aktru Glacier stabilized or even advanced in 1936, 1940, 1969, and 1993, the Malyi Aktru Glacier in 1911, 1936, 1960, 1979, and 1993 [85]. These data are in good agreement with our information on the slowing or halting of retreat of Tavan Bogdo glaciers in the 1990s.

The data of other authors on the retreat of Tavan Bogd glaciers in most cases cover short time intervals and cannot be integrated into our data series, and in some cases, they are inconsistent. For the Potanin glacier it is known that in 1905 the medial moraine and the wedge of the buried ice buried by it reached the moraine of the LIA, dividing the periglacial lake into two parts, but it is not possible to establish the position of the edges of the open ice of the glaciers of Potanin and Alexandra on this data. It is also known that by 1916 this ledge of ice did not change its position, but the open ice experienced a retreat, due to which the lake's dimensions increased. According to [44] in the period from the LIA maximum to 1987 Potanin and Alexandra glaciers retreated by 2000 and 1970 m respectively.. The data of Revyakin and Muhametov were obtained by route observations This is close to our results for the period from the LIA maximum till 1988: 2053 m and 2061 m, respectively. The difference in results could be caused by the difference of methods used.

According to Mikhailov and Ostanin [49], in the period from 1987 to 2001, the Potanin Glacier retreated by 600 m. However, according to our data, the retreat was close to 318 m in the similar period of 1988-2000. The assumption that in two missing years the glacier could retreat to 282 m seems implausible. Probable cause of such difference could be the following – Mihailov and Ostanin [49] obtained their information using the benchmarks installed by Revyakin and Muhametov in 1987, but they admitted that could not restore the information from those benchmarks. Therefore, they probably could misinterpret the distance between the benchmark and the glacial termini in 1987, which could lead to further mistake. On the contrary Syromyatina et al [34] for the similar period of time 1989-2001 reconstructed only 60 m retreat (only 5 m per

year). This is also not very reliable because according to the scientists who visited the glacier in 1987 and 2001 it had a typical for a fast retreating glacier appearance: flat snout without crevasses.

Another estimation of glacial retreat was given by Krumwiede et. al [71] Between 1989 and 2009 Potanin Glacier receded by 516 m, a mean rate of 25.8 m yr^{-1}, and by 5.1% of its total length. Over the same period the adjacent Alexandra Glacier receded by 653 m, a mean rate of 32.7 m yr^{-1}, This is close to our results for 1988-2010 for Potanin Glacier (503 m), but completely different to our estimation of retreat for Alexandra Glacier (349 m). Probably this is due to problems of delineating the front of the glacier, especially due to its progressive moraine coverage.

According to [33] in the interval of 2003-2009 Potanin Glacier retreated about 90 m, average rate 15 m $year^{-1}$, which is in good agreement with our data: 18.5 m $year^{-1}$ in 2000-2010. However, this is quite different to the rapid retreat of Potanin glacier for almost the same period: 180 m from 2001 to 2006 [34]. It is surprising, but the same authors give quite different estimations of the retreat of Potainin glacier for almost the same period: 290 m for 2001-2013 [34] and 364 m (28 m year) for 2001-2014 [72]. This means either a correction of the initial estimations to higher values of retreat or a very high (74 m) retreat of the glacier between 2013 and 2014, which is also possible taking into account our estimations of a rapid glacial retreat in 2010-2018 (tab. 7).

5. Conclusion.

Based on remote sensing data and in situ observations we estimated the LIA glaciation of Tavan Bogd (area 353.4 km^2, average ELA 3235 m), the glacial extent at 1968 (244 km^2) and at 2010 (area 200.98 km^2, average ELA 3285 m). Glacial shrinkage in 1968-2010 was sufficiently faster than in the period between the LIA maximum and 1968. The aspect of the slopes had little effect on the degree of glacier shrinkage, but there was a negative correlation between the size of the glaciers and the rate of degradation. On the background of the general retreat trend large valleys glaciers retreated faster in 1968-1977 and after 2010. In 1990-s the retreat was slow. After 2010 the glacial retreat was extremely fast. Climatic preconditions for this kind of glacier dynamics were the general trend of decrease of precipitation until the mid-1970s, relatively warm conditions in the 1960s-1970s, a cold interval in 1981-1995, and very rapid warming after 1995 were distinguished. Proceeding from this, it is possible to assume the time of the reaction of glaciers to changes in summer temperatures in the range of 9-15 years.

Possible prospects for further work are related to obtaining the latest information on the stepping up of the fronts of the largest Tavan Bogd glaciers, carrying out mass-balance observations and calculations, and also obtaining information on additional time periods by analyzing available images of suitable quality.

Author Contributions

Conceptualization, Dmitry Ganyushkin and Kirill Chistyakov; Data curation, Dmitry Ganyushkin, Dmitry Bantcev and Demberel Otgonbayar; Investigation, Dmitry Ganyushkin and Ilya Volkov; Methodology, Dmitry Ganyushkin, Elena Kunaeva, Tatyana Andreeva and Anton Terekhov; Writing – original draft, Dmitry Ganyushkin.

Conflicts of Interest

The authors declare no conflict of interest.

References

1. Haeberli, W. Glacier Fluctuations and Climate Change Detection. *Geogr. Fis. Dinam. Quat.* 1995, *18*, 191–199.

2. Bahr, D. B.; Dyurgerov, M. B.; Meier, M. F. Sea-level rise from glaciers and ice caps: A lower bound. *Geophys. Res. Lett.* **2009**, doi:10.1029/2008gl036309.

3. Radić, V.; Hock, R. Glaciers in the Earth's Hydrological Cycle: Assessments of Glacier Mass and Runoff Changes on Global and Regional Scales. *Surv. Geophys.* **2014**, *35*, 813–837, doi:10.1007/s10712-013-9262-y.

4. Carey, M. Living and dying with glaciers: People's historical vulnerability to avalanches and outburst floods in Peru. *Glob. Planet. Change* **2005**, *47*, 122–134, doi:10.1016/j.gloplacha.2004.10.007.

5. Rudoy, A. N. Glacier-dammed lakes and geological work of glacial superfloods in the late Pleistocene, southern Siberia, Altai mountains. *Quat. Int.* **2002**, *87*, 119–140, doi:10.1016/S1040-6182(01)00066-0.

6. Chistyakov, K. V; Ganiushkin, D. A. Glaciation and Thermokarst Phenomena and Natural Disasters in the Mountains of North-West Inner Asia. In *Environmental Security of the European Cross-Border Energy Supply Infrastructure*; Culshaw, M. G., Osipov, V. I., Booth, S. J., Victorov, A. S., Eds.; Springer Netherlands: Dordrecht, 2015; pp. 207–218.

7. Meier, M. F.; Roots, E. F. Glaciers as a water resource. *Nat. Resour.* **1982**, *18*, 7–14.

8. Barnett, T. P.; Adam, J. C.; Lettenmaier, D. P. Potential impacts of a warming climate on water availability in snow-dominated regions. *Nature* **2005**, *438*, 303–309.

9. Francou, B.; Coudrain, A. Glacier shrinkage and water resources in the Andes. *Eos, Trans. Am. Geophys. UnionAmerican Geophys. Union* **2005**, *86*, 415.

10. Bradley, R. S.; Vuille, M.; Diaz, H. F.; Vergara, W. Threats to water supplies in the tropical Andes. *Science* **2006**, *312*, 1755–1756.

11. Oerlemans, J. Ectracting a climate signal from 169 gkacier records. *Science (80-.).* **2005**, *308*, 675–677, doi:10.1126/science.1107046.

12. Grove, J. M. *The Little Ice Age*; Methuen: London, 1988;

13. Holzhauser, H.; Zumbühl, H. J. To the history of the Lower Grindelwald Glacier during the last 2800 years — paleosols, fossil wood and pictorical records — new results. *Zeitschrift für Geomorphol. N.F. Suppl. Bd.* **1996**, *104*, 95–127.

14. Lehmkuhl, F. Holocene glaciers in the Mongolian Altai: An example from the Turgen-Kharkhiraa Mountains. *J. Asian Earth Sci.* **2012**, *52*, 12–20, doi:10.1016/j.jseaes.2011.11.027.

15. Patzelt, G. The period of glacier advances in the Alps, 1965 to 1980. *Zeitschrift für Gletscherkd. und Glazialgeol.* **1985**, *21*, 403–407.

16. Zemp, M.; Paul, F.; Hoelzle, M.; Haeberli, W. Alpine glacier fluctuations 1850–2000: An overview and spatio-temporal analysis of available data and its representativity. In *The Darkening Peaks: Glacial Retreat in Scientific and Social Context*; Orlove, B., Wiegandt, E., Luckman, B., Eds.; University of California Press, 2007; pp. 152–167.

17. Zemp, M.; Frey, H.; Gärtner-Roer, I.; Nussbaumer, S. U.; Hoelzle, M.; Paul, F.; Haeberli, W.; Denzinger, F.; Ahlstrøm, A. P.; Anderson, B.; Bajracharya, S.; Baroni, C.; Braun, L. N.; Càceres, B. E.; Casassa, G.; Cobos, G.; Dàvila, L. R.; Delgado Granados, H.; Demuth, M. N.; Espizua, L.; Fischer, A.; Fujita, K.; Gadek, B.; Ghazanfar, A.; Hagen, J. O.; Holmlund, P.; Karimi, N.; Li, Z.; Pelto, M.; Pitte, P.; Popovnin, V. V.; Portocarrero, C. A.; Prinz, R.; Sangewar, C. V.; Severskiy, I.; Sigurdsson, O.; Soruco, A.; Usubaliev, R.; Vincent, C. Historically unprecedented global glacier decline in the early 21st century. *J. Glaciol.* **2015**, *61*, 745–762, doi:10.3189/2015JoG15J017.

18. Zasadni, J. the Little Ice Age in the Alps : Its Record in Glacial Deposits and Rock Glacier Formation. *Landf. Evol. Mt. areas* **2007**, *XLI*, 117–137.

19. Colucci, R. R.; Žebre, M. Late Holocene evolution of glaciers in the southeastern Alps. *J. Maps* **2016**, *12*, 289–299, doi:10.1080/17445647.2016.1203216.

20. Andreassen, L. M.; Elveh??y, H.; Kj??llmoen, B.; Engeset, R. V.; Haakensen, N. Glacier mass-balance and length variation in Norway. *Ann. Glaciol.* **2005**, *42*, 317–325, doi:10.3189/172756405781812826.

21. Stokes, C. R.; Andreassen, L. M.; Champion, M. R.; Corner, G. D. Widespread and accelerating glacier retreat on the Lyngen Peninsula, northern Norway, since their “Little Ice Age” maximum. *J. Glaciol.* **2018**, *64*, 100–118, doi:10.1017/jog.2018.3.

22. Nesje, A.; Bakke, J.; Dahl, S. O.; Lie, Ø.; Matthews, J. A. Norwegian mountain glaciers in the past, present and future. *Glob. Planet. Change* **2008**, *60*, 10–27, doi:10.1016/j.gloplacha.2006.08.004.

23. Rabatel, A.; Francou, B.; Soruco, A.; Gomez, J.; Cáceres, B.; Ceballos, J. L.; Basantes, R.; Vuille, M.; Sicart, J. E.; Huggel, C.; Scheel, M.; Lejeune, Y.; Arnaud, Y.; Collet, M.; Condom, T.; Consoli, G.; Favier, V.; Jomelli, V.; Galarraga, R.; Ginot, P.; Maisincho, L.; Mendoza, J.; Ménégoz, M.; Ramirez, E.; Ribstein, P.; Suarez, W.; Villacis, M.; Wagnon, P. Current state of glaciers in the tropical Andes: A multi-century perspective on glacier evolution and climate change. *Cryosphere* **2013**, *7*, 81–102, doi:10.5194/tc-7-81-2013.

24. Aizen, V. B.; Kuzmichenok, V.; Surazakov, A. B. Glacier changes in central and northern Tien Shan during the last 140 years based on surface and remote sensing data. *Ann. Glaciol.* **2006**, *43*, 202–213.

25. Loibl, D.; Lehmkuhl, F.; Grießinger, J. Reconstructing glacier retreat since the Little Ice Age in SE Tibet by glacier mapping and equilibrium line altitude calculation. *Geomorphology* **2014**, *214*, 22–39, doi:10.1016/j.geomorph.2014.03.018.

26. Kutuzov, S. The retreat of Tien Shan glaciers since the Little Ice Age obtained from the moraine positions, aerial photographs and satellite images. In *PAGES Second Open Science Meeting 10–12 August 2005, Beijing, China.*; 2005.

27. Ganiushkin, D.; Chistyakov, K.; Kunaeva, E. Fluctuation of glaciers in the southeast Russian Altai and northwest Mongolia Mountains since the Little Ice Age maximum. *Environ. Earth Sci.* **2015**, *74*, 1883–1904, doi:10.1007/s12665-015-4301-2.

28. Egorina, A. V.; Popova, K. I.; Dyukarev, A. D.; Kondrat'ev, V. P. *Klimat Yugo-Zapadnogo Altaya (Climate of South-Western Altai).[In Russian].*; Altay State University, East Humanitarian Iinstitute, East--Kazakhstan Center of Hidrometeorology: Ust'-Kamenogorsk, 2002;

29. Ganyushkin, D. A.; Chistyakov, K. V.; Volkov, I. V.; Bantcev, D. V.; Kunaeva, E. P.; Kharlamova, N. F. Modern data on glaciation of the northern slope of Tavan-Bogdo-Ola massif (Altai). *Ice Snow* **2017**, *57*, 307–325, doi:10.15356/2076-6734-2017-3-307-325.

30. Lilun, W.; Chaohai, L.; Ping, W. Modern glaciers in Altai Mountains of China. *Acta Geogr. Sin.* **1985**, *40*, 142–153 (in Chinese with English abstract).

31. LiLun, W. Precipitation condition of glaciated region in Altay mountains in China and its influence on glacial development. In *Conference on glaciology of the geographical society of China (Selection)*; 1990; pp. 64–71.

32. Liu, C. H.; You, G. X.; Pu, J. C. *Glacier Inventory of China II: Altay Mountains (in Chinese).*; Lanzhou Institute of Glaciology and Cryopedology, Academia Sinica: Lanzhou, 1982;

33. Kadota, T.; Gombo, D.; Kalsan, P.; Namgur, D.; Ohata, T. Glaciological research in the Mongolian Altai, 2003-2009. *Bull. Glaciol. Res.* **2011**, *29*, 41–50, doi:10.5331/bgr.29.41.

34. Syromyatina, M. V.; Kurochkin, Y. N.; Chistyakov, K. V.; Ayurzana, C. Current state and changes of glaciers in the Tavan Bogd Mountains (Mongolia). *Ice Snow* **2014**, *54*, 31–38.

35. Sevast'janov, V. V.; Shantykova, L. N. Characteristics of the field of annual precipitation in the Altai Mountains according to glacial climatic parameters (in Russian). *Bull. Tomsk State Univ.* **2001**, *274*, 63–69.

36. Krenke, A. N. Mass exchange in glacier systems on the USSR territory (in Russian, extended English abstract); Hydrometeoizdat: Leningrad, 1982;

37. Sapozhnikov, V. V. Mongolian Altai in the sources of the Irtysh and Kobdo. Travels of 1906-1911; Empire Tomsk University: Tomsk, 1911;

38. Tronov, B. V.; Tronov, M. V. Investigations in the Southern Altai - a short report on trips to the Altai in 1912, 13, 15 and 16. *Bull. Tomsk State Univ.* **1924**, *24*, 210.

39. Tronov, B. V. Catalog of Altai Glaciers. *Bull. Russ. Geogr. Soc.* **1925**, *57*, 107–159.

40. Revyakin, V. S.; Okishev, P. A. Present-day glaciation of r. Argut upper basin. *Glaciol. Altai* **1970**, *6*, 29–36 (in Russian).

41. Katalog lednikov SSSR. The USSR Glacier Inventory. **1977**, *15*, 47 (in Russian).

42. Revyakin, V. S.; Muhametov, R. M. Dinamika lednikov Altae-Sanskoj gornoj sistemy za 150 let. Dynamics of the glaciers of Altai-Sayan mountain system over the last 150 years. *Data Glaciol. Stud.* **1986**, *57*, 95–99 (in Russian).

43. Bjamba, Z.; Selivanov, E. I. Present glaciation of Mongolia. *Bull. All-Union Geogr. Soc.* **1971**, *103*, 249–254 (in Russian).

44. Revyakin, V. S.; Muhametov, R. M. Dynamics of the glaciers of Tabyn-Bogdo-Ola. *Glaciol. Sib.* **1993**, *19*, 83–92 (in Russian).

45. Seliverstov, Y. P.; Moskalenko, I. G.; Chistyakov, K. V. Glaciation of the northern slope of Tavan-Bogdo-Ola massif and its dynamics. *Proc. Russ. Geogr. Soc.* **2003**, *135*, 1–16 (in Russian).

46. Chistyakov, K. V.; Moskalenko, I. G. Glaciation of the northern slope of Tabyn-Bogdo-Ola Massif and its dynamics. *Data Glaciol. Stud.* **2006**, *101*, 111–116 (in Russian).

47. Moskalenko, I. G.; Ganyushkin, D. A.; Chistyakov, K. V. Modern and ancient glaciation of northern slope of the Tavan-Bogdo-Ola massif. *Ice Snow* **2013**, *53*, 33–44 (in Russian).

48. Ganyushkin, D. A.; Chistyakov, K. V.; Volkov, I. V.; Bantsev, D. V.; Kunaeva, E. P.; Kharlamova, N. F. Modern data on glaciation of the northern slope of Tavan-Bogdo-Ola massif (Altai). *Led i Sneg* **2017**, *57*, doi:10.15356/2076-6734-2017-3-307-325.

49. Mihajlov, N. N.; Ostanin, O. V. Glaciers of the South and Mongolian Altai and their changes in the 20th century. *Geogr. Nat. Manag. Sib.* **2002**, *5*, 3–20.

50. Kadota, T.; Davaa, G. Recent glacier variations in Mongolia. *Ann. Glaciol.* **2007**, 185–188.

51. Konya, K.; Kadota, T.; Nakazawa, F.; Davaa, G.; Kalsan, P.; Yabuki, H.; Ohata, T. Surface mass balance of the Potanin Glacier in Mongolian Altai Mountains and comparison with Russian Altai glaciers in 2005, 2008 and 2009. *Bull. Glaciol. Res.* **2013**, *31*, 9–18.

52. Nakazawa, F.; Konya, K.; Kadota, T.; Ohata, T. Depositional and summer snow melting features in 2007–2011 on the upstream side of Potanin Glacier, Mongolian Altai, reconstructed by pollen and oxygen isotope analysis. *Environ. Earth Sci.* **2015**, *74*, 1851–1859, doi:10.1007/s12665-015-4436-1.

53. Kamp, U.; Krumwiede, B.; Mcmanigal, K.; Pan, C.; Walther, M.; Dashtseren, A. *The Glaciers of Mongolia*; Denver, CO, USA: Denver, CO, USA, 2013;

54. Kamp, U.; Pan, C. G. Inventory of glaciers in Mongolia, derived from Lanfsat imagery from 1989 to 2011. *Geogr. Ann. Ser. A, Phys. Geogr.* **2015**, *97*, 653–669, doi:10.1111/geoa.12105.

55. Guo, W.; Liu, S.; Xu, J.; Wu, L.; Shangguan, D.; Yao, X.; Wei, J.; Bao, W.; Yu, P.; Liu, Q.; Jiang, Z. The second Chinese glacier inventory: Data, methods and results. *J. Glaciol.* **2015**, *61*, 357–372, doi:10.3189/2015JoG14J209.

56. Krumwiede, B. S.; Kamp, U.; Leonard, G. J.; Kargel, J. S.; Dashtseren, A.; Walther, M. Recent Glacier Changes in the Mongolian Altai Mountains: Case Studies from Munkh Khairkhan and Tavan Bogd. In *Global Land Ice Measurements from Space*; Kargel, J. S., Leonard, G. J., Bishop, M. P., Kääb, A., Raup, B. H., Eds.; Springer Berlin Heidelberg: Berlin, Heidelberg, 2014; pp. 481–508 ISBN 978-3-540-79818-7.

57. Kurowsky, L. Die Hohe der Schneegrenze mit besonderer Berucksichtigung der Finsteraargorngruppe. *Pencks Geogr. Abhandlungen* **1891**, *5*, 115–160 (in German).

58. Glazyrin, G. E. *Distribution and Regime of Mountain Glaciers*; Hydrometeoizdat: Leningrad, 1985;

59. Labutina, L. A. *nterpretation of Aerospace Images. Manual.*; Aspekt-Press: Moscow, 2004;

60. Akovetskii, V. I. *Image Interpretation*; Nedra: Moscow, 1983;

61. Blomdin, R.; Heyman, J.; Stroeven, A. P.; Haettestrand, C.; Harbor, J. M.; Gribenski, N.; Jansson, K. N.; Petrakov, D. A.; Ivanov, M. N.; Alexander, O.; Rudoy, A. N.; Walther, M. Glacial geomorphology of the Altai and Western Sayan Mountains, Central Asia. *J. Maps* **2016**, *12*, 123–136, doi:10.1080/17445647.2014.992177.

62. Ganyushkin, D. A.; Kunaeva, E. P.; Chistyakov, K. V.; Volkov, I. V. Interpretation of Glaciogenic Complexes From Satellite Images of the Mongun-Taiga Mountain Range. *Geogr. Nat. Resour.* **2018**, *39*, doi:10.1134/S1875372818010092.

63. Ganyushkin, D. A.; Chistyakov, K. V.; Kunaeva, E. P.; Volkov, I. V.; Bantsev, D. V. Current glaciation of the Chikhachev ridge (South-Eastern Altai) and its dynamics after maximum of the Little Ice Age. *Ice Snow* **2016**, *56*, 29–42 (in Russian), doi:10.15356/2076-6734-2016-1-29-42.

64. Chistyakov, K. V.; Ganushkin, D. A.; Moskalenko, I. G.; Dullo, W.-C. The glacier complexes of the mountain massifs of the north-west of Inner Asia and their dynamics. *Geogr. Environ. Sustain.* **2011**, *4*, 4–21.

65. Ganyushkin, D. A. Glacigenic complexes of sharply continental area of north-west Inner Asia., Saint-Petersburg state university: Saint-Petersburg, 2015.

66. Ganyushkin, D. A.; Otgonbayar, D.; Chistyakov, K. V.; Kunaeva, E. P.; Volkov, I. V. Recent glacierization of the Tsambagarav ridge (North Western Mongolia) and its changes since the Little Ice Age maximum. *Ice Snow* **2016**, *56*, 437–452, doi:10.15356/2076-6734-2016-4-437-452.

67. Ganyushkin, D. A.; Chistyakov, K. V.; Volkov, I. V.; Bantcev, D. V.; Kunaeva, E. P.; Terekhov, A. V. Present glaciers and their dynamics in the arid parts of the altai mountains. *Geosci.* **2017**, *7*, doi:10.3390/geosciences7040117.

68. Revyakin, V. S.; Muhametov, R. M. Dynamics of the glaciers of Altai-Sayan mountain system over the last 150 years. *Data Glaciol. Stud.* **1986**, *57*, 95–99 (in Russian).

69. Ganyushkin, D. A.; Chistyakov, K. V.; Volkov, I. V.; Bantcev, D. V.; Kunaeva, E. P. Present dynamics of the glaciers of arid areas of Altai and different patterns of glacial retreat. *Geosciences* **2017**.

70. Galakhov, V. P.; Red'kin, A. G. Sovremennoe i drevnee oledenenie gornogo uzla Tabyn-Bogdo-Ola. Present and past glaciation of Tavan Bogd mountain knot. *Geogr. i Prir. Sib.* **2001**, 153–175 (in Russian).

71. Krumwiede, B. S.; Kamp, U.; Leonard, G. J.; Kargel, J. S.; Dashtseren, A.; Walther, M. Recent glacier changes in the Mongolian Altai Mountains: Case studies from Munkh Khairkhan and Tavan Bogd. *Glob. L. Ice Meas. from Sp.* **2014**, *2*.

72. Syromyatina, M. V.; Kurochkin, Y. N.; Bliakharskii, D. P.; Chistyakov, K. V. Current dynamics of glaciers in the Tavan Bogd Mountains (Northwest Mongolia). *Environ. Earth Sci.* **2015**, *74*, 1905–1914, doi:10.1007/s12665-015-4606-1.

73. Cogley, G. (submitter); Gardner, A.; Cogley, G.; Earl, L.; Raup, B. H. (analyst(s)) GLIMS Glacier Database. In; National Snow and Ice Data Center: Boulder, C.O., 2015.

74. Earl, L.; Gardner, A. A satellite-derived glacier inventory for North Asia. *Ann. Glaciol.* **2016**, *57*, 50–60, doi:10.3189/2016AoG71A008.

75. Shiyin, L. I. U. The 2nd Glacier Inventory of China. **2009**, *50*, 1–4.

76. Zemp, M.; Paul, F.; Hoelzle, M.; Haeberlie, W. Glacier Fluctuations in the European Alps, 1850-2000: An overview and spatio-temporal analysis of available data. *Darkening Peaks Glacial Retreat Sci. Soc. Context* **2006**, doi:10.5167/uzh-9024.

77. Kutuzov, S.; Shahgedanova, M. Glacier retreat and climatic variability in the eastern Terskey-Alatoo, inner Tien Shan between the middle of the 19th century and beginning of the 21st century. *Glob. Planet. Change* **2009**, *69*, 59–70, doi:10.1016/j.gloplacha.2009.07.001.

78. Ganiushkin, D.; Chistyakov, K.; Kunaeva, E. Fluctuation of glaciers in the southeast Russian Altai and northwest Mongolia Mountains since the Little Ice Age maximum. *Environ. Earth Sci.* **2015**, *74*, doi:10.1007/s12665-015-4301-2.

79. Liu, S.; Junli, X.; Guo, W.; Zhang, S. Glaciers in China and Their Variations. In *Global Land Ice Measurements from Space*; 2014; pp. 583–608 ISBN 978-3-540-79817-0.

80. Wang, S. H.; Xie, Z. C.; Dai, Y. N.; Liu, S. Y.; Wang, X. Structure, change and its tendency of glacier systems in Altay Mountains. *Arid L. Geogr.* **2011**, *34*, 115–123.

81. Wang, P.; Li, Z.; Luo, S.; Bai, J.; Huai, B.; Wang, F.; Li, H.; Wang, W.; Wang, L. Five decades of changes in the glaciers on the Friendship Peak in the Altai Mountains, China: Changes

in area and ice surface elevation. *Cold Reg. Sci. Technol.* **2015**, *116*, 24–31, doi:10.1016/j.coldregions.2015.04.002.

82. Solomina, O. N. Retreat of mountain glaciers of northern Eurasia since the Little Ice Age maximum. **2000**.

83. Dushkin, M. A. Long-term fluctuations of the Aktru glaciers and the conditions for the development of young moraines. *Glaciol. Altai* **1965**, *4*, 83–101 (in Russian).

84. Narozhnyj, J. K.; Nikitin, S. A. The modern glaciation of Altai at the turn of the 21st century. *Data Glaciol. Stud.* **2003**, *95*, 93–11 (in Russian).

85. Narozhnyj, J. K. Resource assessment and trends in glacier change in the Aktru basin (Altai) over the past century and a half. *Data Glaciol. Stud.* **2001**, *90*, 117–125 (in Russian).